

*****RMIS Viewprint Document Cover Sheet*****

This document was retrieved from the Records Management Information System (RMIS). It is intended for information only and may not be the most recent or updated version.

Accession #: **D5449056**

Document #: **RPP-21695**

Title/Desc:

**LITERATURE SURVEY FOR FRACTIONAL CRYSTALLIZATION
STUDY**

Pages: **42**

JUL 14 2004
24

S

ENGINEERING DATA TRANSMITTAL

1. EDT 820947
1A. Page 1 of 1

2. To: (Receiving Organization) Distribution	3. From: (Originating Organization) Analytical Process Development	4. Related EDT No.: NA
		7. Purchase Order No.: NA
5. Proj./Prog./Dept./Div.: Analytical Technical Services	6. Design Authority/Resp. Engr./Design Agent: J. C. Person	9. Equip./Component No.: NA
		10. System/Bldg./Facility: 222-S
8. Originator Remarks: This document is being released into the supporting document system for retrievability purposes.		12. Major Assembly Dwg. No.: NA
		13. Permit/Permit Application No.: NA
11. Receiver Remarks: NA	11A. Design Basis Document? <input type="checkbox"/> Yes <input checked="" type="checkbox"/> No	14. Required Response Date: 6/30/04

15. DATA TRANSMITTED					(F)	(G)	(H)	(I)
(A) Item No.	(B) Document/Drawing No.	(C) Sheet No.	(D) Rev. No.	(E) Title or Description of Data Transmitted	Approval Designator	Reason for Transmittal	Originator Disposition	Receiver Disposition
1	RPP-21695	NA	0	Literature Survey for Fractional Crystallization Study	NA	2	1	1

16. KEY

Approval Designator (F) See TFC-ESHQ-Q-INSP-C-05	Reason for Transmittal (G) 1. Approval 2. Review 3. Post-Review	Disposition (H) & (I) 1. Approved 2. Approved w/comment 3. Reviewed no comment 4. Reviewed w/comment 5. Disapproved
--	---	---

17. SIGNATURE/DISTRIBUTION

(G) Reason	(H) Disp.	(J) Name	(K) Signature	(L) Date	(M) MSIN	(G) Reason	(H) Disp.	(J) Name	(K) Signature	(L) Date	(M) MSIN
		Design Auth.				3	1	K. A. Gasper		7/8/04	H6-03
1	1	Resp. Engr. J. C. Person	<i>J.C. Person</i>	6/28/04	T6-07		1	D. L. Herting	<i>D.L. Herting</i>	6/28/04	T6-07
1	1	Resp. Mgr. C. M. Seidel	<i>Cary M Seidel</i>		T6-14						
		QA									
		Safety									
		Env.									
		Design Agent									

18. Signature of EDT Originator <i>J.C. Person</i> Date: 6/28/04	19. DOE APPROVAL (if required) Ctrl. No.	20. Design Authority/Resp. Engr./Resp. Mgr. <i>Cary M Seidel</i> Date: 6/28/04
--	---	--

Literature Survey for Fractional Crystallization Study

J. C. Person

CH2M HILL Hanford Group, Inc.

Richland, WA 99352

U.S. Department of Energy Contract DE-AC27-99RL14047

EDT/ECN: 820947

UC:

Cost Center: 7S110

Charge Code:

B&R Code:

Total Pages: 41

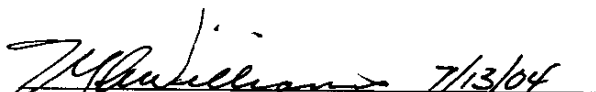
Key Words:

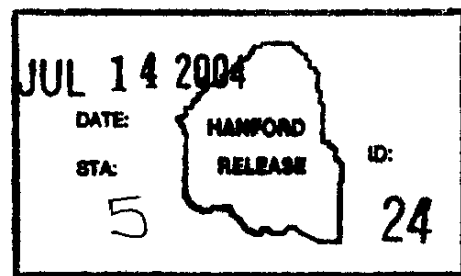
Abstract:

The literature survey fulfills the requirements of the Test Plan for Tank 241-S-112 Fractional Crystallization Study, RPP-18541.

TRADEMARK DISCLAIMER. Reference herein to any specific commercial product, process, or service by trade name, trademark, manufacturer, or otherwise, does not necessarily constitute or imply its endorsement, recommendation, or favoring by the United States Government or any agency thereof or its contractors or subcontractors.

Printed in the United States of America. To obtain copies of this document, contact: Document Control Services, P.O. Box 950, Mailstop H6-08, Richland WA 99352, Phone (509) 372-2420; Fax (509) 376-4989.


Release Approval 7/13/04
Date



Release Stamp

Approved For Public Release

RPP-21695
Revision 0

LITERATURE SURVEY FOR FRACTIONAL CRYSTALLIZATION STUDY

J. C. Person
CH2M HILL Hanford Group, Inc.

Date Published
June 2004



CH2MHILL
Hanford Group, Inc.

Prepared for the U.S. Department of Energy
Office of River Protection

Contract No. DE-AC27-99RL14047

**LITERATURE SURVEY FOR
FRACTIONAL CRYSTALLIZATION STUDY**

CONTENTS

INTRODUCTION	1
1. FRACTIONAL CRYSTALLIZATION DESIGN.....	2
2. FRACTIONAL CRYSTALLIZATION IN THE NaNO_3 - CH_3COONa - H_2O SYSTEM....	6
3. Na_2CO_3 - Na_2SO_4 - H_2O SYSTEM.....	9
4. SOLUBILITIES AND OTHER TOPICS	13
5. COMPARISONS WITH THERMODYNAMIC CALCULATIONS.....	15
6. CRYSTALLIZATION SYSTEMS AND CRYSTALLIZERS	23

INTRODUCTION

The literature survey for the fractional crystallization study of material from tank 241-S-112 is completed, fulfilling the requirements of the *Test Plan for Tank 241-S-112 Fractional Crystallization Study* (Herting 2003).

Crystallization involves the formation of one or more solid phases from a fluid phase or an amorphous solid phase. It is applied extensively in the chemical industry, both as a purification process and a separation process. The main advantage of crystallization over distillation is the production of substances with a very high purity, at a low level of energy consumption, and at relatively mild process conditions. Crystallization is one of the older operations in the chemical industry; therefore, practical experience can usually be used for the design and operation of industrial crystallizers. In addition, advances in the understanding of crystallization kinetics can be useful in the control, design, and scale-up of industrial crystallizers.

Research work is currently underway; e.g., the CrysCODE (Crystallizer COnTrol & Design) project, <http://www.api.tudelft.nl/project/Cryscodex/cryscodex.htm>, at the Delft University of Technology, with the goal of improving the performance and controllability of industrial crystallizers by means of better control and improved design methodologies. Recent developments in fluid dynamics and reactor technology (e.g., compartment approaches) have led to a better understanding of processes and scale-up phenomena.

The ultimate aim of such research is to develop a knowledge-based design frame for optimization of industrial crystallization units. Development work is in progress on a rigorous design analysis model for the description of the crystallization process as a function of the reactor geometry, crystallization kinetics, and operating conditions. One modeling effort is aimed at improving the predictive crystallizer model by implementing a population balance equation that depends on two variables: the size and strain of the crystal. Both the crystal size and the strain in the crystal lattice have a pronounced effect on the growth rate of the individual crystals (Menon 2003).

This report is organized into six sections. Section 1 summarizes reports on the design principles for separations by crystallization. Section 2 discusses the fractional crystallization in the NaNO_3 - CH_3COONa - H_2O system presented in RPP-18541, "Test Plan for Tank 241-S-112 Fractional crystallization Study," dated 2003. Section 3 summarizes reports on crystallization in the Na_2CO_3 - Na_2SO_4 - H_2O system, which includes the effects of the burkeite double salt ($\text{Na}_2\text{CO}_3 \cdot 2\text{Na}_2\text{SO}_4$). Section 4 summarizes solubility data for sodium compounds and presents two miscellaneous topics. Section 5 is excerpted from the internet to show applications of thermodynamic calculations. Section 5.1 compares results and calculations for the NaNO_3 - Na_2SO_4 - H_2O system, and Section 5.2 shows the use of the calculations to optimize flowsheets. Flowsheets are given for two examples: (1) the production of KNO_3 from NaNO_3 and KCl (including the effects of having Na_2SO_4 in the initial material) and (2) the production of K_2SO_4 and NaCl from Na_2SO_4 and KCl . Section 6 is excerpted from the internet to show some examples of the information available on crystallizers.

Section 1 through Section 4 are organized with the citations listed first in bold type, followed by a summary of the paper.

1. FRACTIONAL CRYSTALLIZATION DESIGN

Fractional crystallization effects separations by manipulating the relative solubilities of the components in a solution by solvent addition/removal, stream combination, and heating/cooling. The technique is used to separate a wide variety of chemicals. For example, minerals such as borax, lithium sulfate monohydrate, potash, sodium carbonate, and sodium chloride are crystallized from brines (Hightower 1951; Mehta 1988; Jongema 1993). An early discussion of the methods using temperature and solvent swings to effect crystallization is given in Purdon and Slater (1946), with Mullin (1993) giving an abbreviated version. Five papers are summarized here that discuss the design of fractional crystallization processes (Fitch 1970, Cisternas and Rudd 1993, Dye and Ng 1995, Berry and Ng 1996, Thomsen et al. 1998). Additional papers on the design of fractional crystallization processes include Rajagopal et al. (1988) and Ng (1991).

The fractional crystallization flowsheet employs evaporative crystallizers, thereby restricting the process compositions to isothermal slices of the phase diagram. This distinguishes it from extractive crystallization, a multi-component separation process in which only cooling crystallization is used (Dye and Ng 1995a; Rajagopal 1991). Fractional crystallization is sometimes considered synonymous with melt crystallization (Gilbert 1991). Melt crystallization is the separation process by which fractional separation is effected by directional solidification from the melt, usually without the use of solvents.

1.1 **Dye, S. R., and K. M. Ng, 1995, "Fractional Crystallization: Design Alternatives and Tradeoffs," *AIChE J.*, **41**, 2427-38.**

Guidelines for the design of fractional crystallization processes to separate two and three-solute mixtures are presented. These processes use solvent addition/removal, stream combination, and heating/cooling to bypass regions of multiple saturation in the phase diagram and recover pure solutes. The design equations are formulated, and the constraints on the design variables are identified. The effect on recycle flows of changes in the design variables and an estimate of the cost of separation is also discussed. This work differs from earlier discussions (Fitch 1970; Cisternas and Rudd 1993) of fractional crystallization design, which are based on multiple saturation points at which co-crystallization of two or more compounds occurs. While this simplifies the design procedure, it may be inadvisable because avoidance of co-crystallization is critical to produce pure products. The focus is on separation of binary and ternary mixtures that do not form hydrates or compounds.

Some conclusions are now summarized. Based on the relative positions of the double-saturation points at two different temperatures, a single flowsheet configuration allows the complete separation of two-solute mixtures. The three-solute phase diagrams are characterized by the overlaps between different regions at different temperatures. If the appropriate overlaps exist, it is feasible to separate the three solutes using a one-loop scheme with two or more isotherms. Otherwise, two-loop schemes are necessary. A case study of a one-loop, three solute separation

estimates the costs. Two solute characteristics are desirable. Solutes with high solubilities minimize the amount of solvent vaporized. Solutes with high freezing points make refrigeration unnecessary. Fractional crystallization is expected to play a more significant role in future separations because of the greater need to minimize waste disposal and to reduce the loss of desirable products.

1.2 Thomsen, K., P. Rasmussen, and R. Gani, 1998, "Simulation and Optimization of Fractional Crystallization Processes," *Chem. Eng. Sci.*, 53, 1551-1564.

A general method for the calculation of various types of phase diagrams for aqueous electrolyte mixtures is outlined. It is shown how the thermodynamic equilibrium precipitation process can be used to satisfy the operational needs of industrial crystallizer/centrifuge units. Examples of simulation and optimization of fractional crystallization processes are shown (Section 5.2 shows two of these examples).

The optimization of fractional crystallization processes requires a detailed knowledge of the phase equilibria for such processes. The use of phase diagrams based on experimental data alone will be of limited scope due to the limited data available. Berry and Ng (1996) recognized the need for phase diagrams at various temperatures for design of fractional crystallization processes, but their method requires a prior knowledge of activity coefficients. This paper uses phase diagrams calculated using a thermodynamic model to describe the highly non-ideal aqueous electrolyte systems.

1.3 Berry, D. A., and K. M. Ng, 1996, "Separation of Quaternary Conjugate Salt Systems by Fractional Crystallization," *AIChE J.*, 42, 2162-74.

A method that synthesizes fractional crystallization separation processes to obtain pure solids from conjugate salt solutions (a quaternary conjugate salt system is formed by dissolving two salts without a common ion in an inert solvent) is presented. The method includes a procedure to generate phase diagrams by using solubility products, and it explains how to calculate component concentrations at points on a projection of the phase diagram (the Jänecke projection). Three separation classes are identified for solutions from which only simple salts crystallize. Process paths and design equations are given for each class. Also, the method is applicable to systems in which hydrates and double salts are present. An example projection is given for a system from which AX, BY, AY, BX, AY·3BY, AY·H₂O, AY·AX·H₂O may precipitate, based on the NaNO₃ - K₂SO₄ - H₂O system. The solubility products require knowledge of activity coefficients, which can be calculated using thermodynamic models (e.g., the papers of Thomsen and coworkers in Section 5 and Nicolaisen et al. 1993).

1.4 Cisternas, L. A., and D. F. Rudd, 1993, "Process Design for Fractional Crystallization from Solution," *Ind. Eng. Chem. Res.*, 32, 1993-2005.

A systematic procedure for the identification of alternative process designs for fractional crystallization from solution is presented. The authors seek designs with low rates of recycle, evaporation, and dilution. Only a limited number of designs needs to be analyzed if the crystallizations are operated at hot and cold points of multiple saturation and if the salts are

ordered so that the relative composition is greater at the cold point than at the hot point. Systems are examined that form (1) anhydrous and hydrated single salts, (2) anhydrous and hydrated, congruently soluble, multiple salts, and (3) anhydrous and hydrated, incongruently soluble, multiple salts. The paper states that systems that form solid solutions (e.g., those in Fitch 1976) and systems that do not have sufficiently temperature-dependent equilibria can be considered as simple extensions of the general principles.

Expressions are given for material balances for the techniques discussed by Fitch (1970). Examples are also presented. One example is the separation of burkeite from sodium carbonate and sodium sulfate. This system does not form a double salt below 30 °C. Above 30 °C, burkeite forms. Table 1.1 shows data (Linke 1965) for points of multiple saturation for this system. The last column shows the relative composition, R, which is the mass ratio of salt 1 to salt 2. The system is incongruently soluble. Several processes are possible for separating burkeite. First, two temperatures can be selected below 30°C, for example, 15 °C and 25 °C. This choice leads to designs IA and IB, with IA preferred because of its lower evaporation, dilution, and recycle flows.

Table 1.1. Points of Multiple Saturation in Na₂CO₃ - Na₂SO₄ - H₂O System.

T °C	Solution Composition Wt %		Solid Phase	R
	Na ₂ CO ₃	Na ₂ SO ₄		
15	12.3	8	Na ₂ CO ₃ ·10H ₂ O + Na ₂ SO ₄ ·10H ₂ O	0.65
20	14.95	11.2	Na ₂ CO ₃ ·10H ₂ O + Na ₂ SO ₄ ·10H ₂ O	0.75
25	17.9	16.2	Na ₂ CO ₃ ·10H ₂ O + Na ₂ SO ₄ ·10H ₂ O	0.91
30	25.8	8.6	Na ₂ CO ₃ ·10H ₂ O + burkeite	0.33
	15.5	19.5	Burkeite + Na ₂ SO ₄	1.26
	10.2	25.1	Na ₂ SO ₄ + Na ₂ SO ₄ ·10H ₂ O	2.46
50	29.7	5.5	Na ₂ CO ₃ ·H ₂ O + burkeite	0.19
	11.4	22.2	Burkeite + Na ₂ SO ₄	1.95

Another possibility is to choose a cold temperature where burkeite does not form and a hot temperature where burkeite forms; e.g., 20 °C and 50 °C. This choice leads to designs IIA1 and IIB1, with IIB1 preferred because of its lower evaporation, dilution, and recycle flows. It is also possible to choose both temperatures where burkeite forms; e.g., 30 °C and 50 °C. This choice leads to eight designs, with two preferred because of their lower evaporation, dilution, and recycle flows. Flow diagrams are given in the paper for the four preferred designs, but it is not possible to distinguish between the four designs based only on material balance.

1.5 Fitch, B., 1970, "How to Design Fractional Crystallization Processes," *Ind. Eng. Chem.*, 62(12), 6-33.

One of the most comprehensive discussions of fractional crystallization design is provided. This review covers the basic operations to effect separation, such as heating/cooling. It also covers

examples of various phase behaviors for systems with hydrate or compound formation, solutions of salts with a common ion, and systems of conjugate salts. However, these designs are based on multiple saturation points at which co-crystallization of two or more compounds occurs.

The paper presents a set of systemized procedures by which ideal equilibrium processes can be generated from solubility data. It first treats three-component systems, then four-component systems, and ending with n-component systems.

1.6 Extractive Crystallization and Melt Crystallization

The next three papers are concerned with separations by two specialized types of crystallization. Extractive crystallization is a multi-component separation process in which only cooling crystallization is used. Melt crystallization is the separation process by which fractional separation is effected by directional solidification from the melt, usually without the use of solvents.

1.6.1 Dye, S. R., and K. M. Ng, 1995a, "Bypassing Eutectics with Extractive Crystallization: Design Alternatives and Tradeoffs," *AIChE J.*, 41, 1456-70.

A systematic design method to use extractive crystallization to separate a three-solute mixture despite the presence of eutectics is presented. Phase behavior is classified into six basic types. Design equations are formulated for these six flowsheet structures, and the design variables and constraints are identified. A discussion of design issues and an estimate of the costs are also included.

1.6.2 Rajagopal, S., K. M. Ng, and J. M. Douglas, 1991, "Design and Economic Trade-Offs of Extractive Crystallization Processes," *AIChE J.*, 37, 437-47.

A systematic procedure for the separation of a binary mixture by means of extractive crystallization is presented. Two flowsheet structures are given to cover a wide variety of phase behaviors. Design equations are formulated for both flowsheet structures, and the design variables and constraints are identified.

1.6.3 Gilbert, S. W., 1991, "Melt Crystallization: Process Analysis and Optimization," *AIChE J.*, 37, 1205-18.

Melt crystallization manufacturing systems are characterized mathematically and optimized. Directional solidification and sweating are modeled, and the results are correlated to plant data. An algorithm is constructed to determine the optimal design and operation of a production plant. The models were developed to optimize two melt crystallization operations: static and dynamic.

The directional solidification from the melt can be done in several ways: falling-film, shell-and-tube, cone, scraped surface, roll, screw and weir crystallizers, zone refiners, sweated pan apparatus, and crystal washing devices.

2. FRACTIONAL CRYSTALLIZATION IN THE NaNO₃ - CH₃COONa - H₂O SYSTEM

2.1 Krapukhin, V. B., E. P. Krasavina, and A. K. Pikaev, 1997, *Crystallization of Sodium Nitrate from Radioactive Waste*, PNNL-11616, Pacific Northwest National Laboratory, Richland, Washington.

Scientists at the Institute of Physical Chemistry of the Russian Academy of Sciences have performed extensive work on fractional crystallization of radioactive tank waste (Krapukhin 1997). Their separation of sodium nitrate and sodium acetate is an elegant example of the importance of understanding phase diagram relationships in designing a successful flowsheet.

Figure 2.1 shows a phase diagram of the equilibria of NaNO₃ - CH₃COONa - H₂O mixtures, with the concentrations plotted as weight percentages (wt %).

Analysis of the phase diagram was used to design flowsheets of operations to separate the sodium nitrate and sodium acetate. The phase diagram shows that a single crystallization will not give a salt yield of more than 50% to 60% of the amount of salt in the initial solution. However, repeated recycling of the mother liquor solutions from crystallization to the beginning of the process could produce yields near 100%.

Two flowsheets were designed, depending on the relative abundances of the two species. Figure 2.2 shows the flowsheet for solutions rich in sodium acetate. Figure 2.3 schematically shows the separation for solutions rich in sodium nitrate, with the flowsheet shown in Figure 2.4. (The four figures are taken directly from the referenced document, without alteration.)

The shaded areas of Figure 2.3 represent regions in which crystallization of one salt is possible (NaNO₃ in the lower left region at 70 °C, NaC₂H₃O₂·3H₂O in the upper right region at 20 °C). Consider a dilute feed solution at point P₁, containing 91% water, 5% NaNO₃, and 4% NaC₂H₃O₂ by weight. As the solution is evaporated at 70 °C, its composition moves along the line O-M until it reaches point F, where NaNO₃ begins to precipitate.

Further evaporation causes more NaNO₃ to precipitate, and the composition of the solution moves along line n₂-Q until it reaches point Q. At that point, the crystals are harvested. Water is added to the solution to move the solution composition along line N-O from point Q to point A, and the solution is cooled to 20 °C to induce precipitation of NaC₂H₃O₂·3H₂O. As the acetate salt precipitates, the solution composition moves from point A to point C, at which point the crystals are harvested. From point C, the process is repeated – heating and evaporating to point F, harvesting NaNO₃ at point Q, diluting and cooling to point A, harvesting NaC₂H₃O₂·3H₂O at point C, and so on until the salts have been separated.

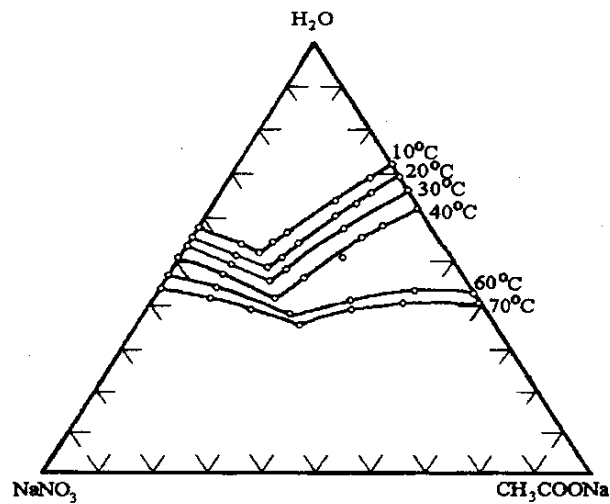


Figure 2.1. Phase Composition Diagram for NaNO_3 - CH_3COONa - H_2O System.

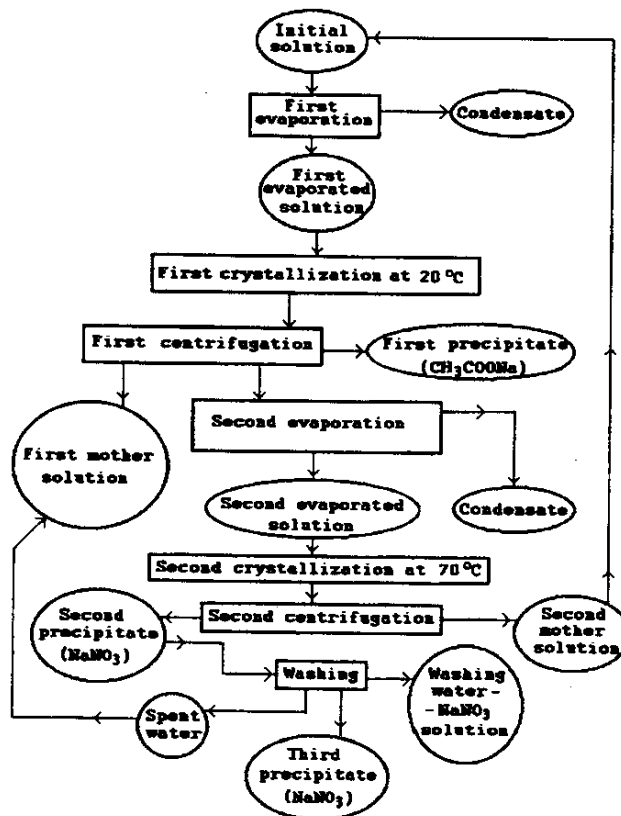


Figure 2.2. Flowsheet for Separation from Waste Solutions Rich in Sodium Acetate.

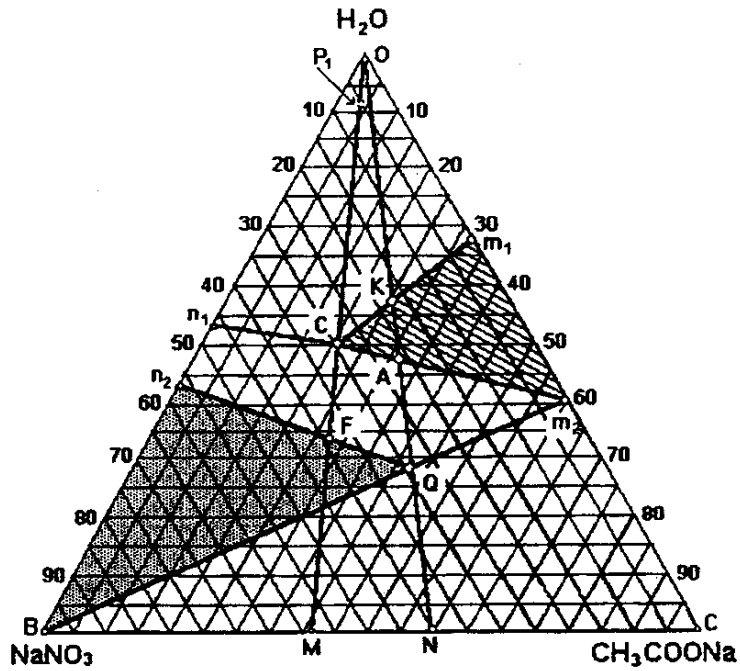


Figure 2.3. Sodium Nitrate / Sodium Acetate Phase Diagram (wt %).

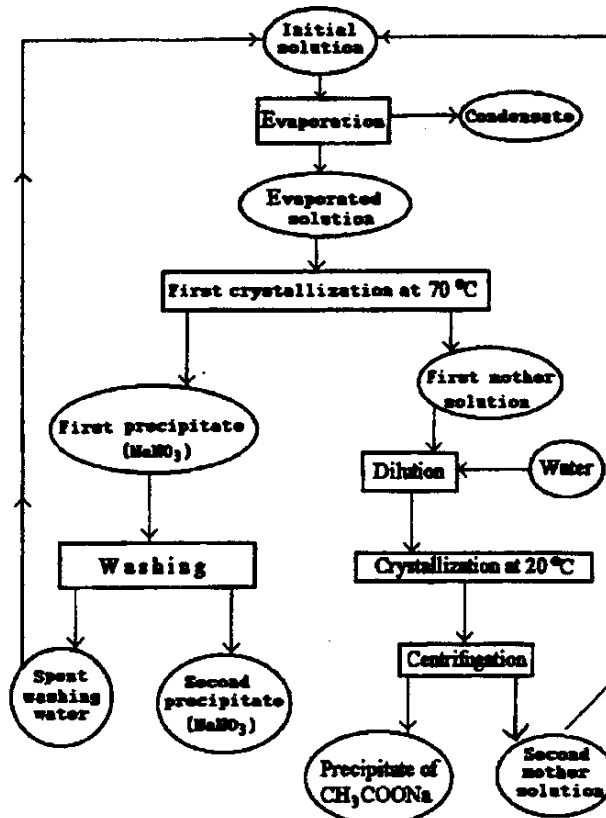


Figure 2.4. Flowsheet for Separation from Waste Solutions Rich in Sodium Nitrate.

3. Na_2CO_3 - Na_2SO_4 - H_2O SYSTEM

3.1 Shi, B., and R. W. Rousseau, 2003, "Structure of Burkeite and a New Crystalline Species Obtained from Solutions of Sodium Carbonate and Sodium Sulfate," *J. Phys. Chem.*, **B107**, 6932-37.

This paper examines and explains the variation of burkeite composition and identifies a new double salt containing approximately 2 moles of Na_2CO_3 per mole of Na_2SO_4 . The new species was formed at 115 °C from solutions with composition mole ratios of Na_2CO_3 to Na_2SO_4 ranging from approximately 5 to 7.

The carbonate-to-sulfate molar ratio (C:S) for burkeite is nominally 1:2. However, previous workers found considerable variation in the C:S ratio for burkeite, e.g., 1:1.9 (Forshag 1935), 1:1 to 1:3 (Schroeder 1936), and 1:1.4 to 1:2.2 (Green and Frattali 1946).

Crystals formed by evaporation were filtered and washed to remove interstitial liquid. A washing protocol was developed using five wash liquids, containing various mixtures of ethylene glycol, water, and ethanol. The first substantial crop of crystals to form at each mixture was identified by X-ray powder diffraction (XRD). Also, a scanning electron microscope (SEM) was used to examine the crystal structures, and the SEM included an energy-dispersive X-ray spectroscopy (EDS) system. The composition of the crystals was analyzed using an automatic titrator.

Evaporative crystallization studies were conducted using solutions that had carbonate-to-sulfate molar ratios in the liquid (C:S-liq) from 1:5 to 12:1 (the carbonate mole fraction in the liquid, not counting the moles of water, from 0.17 to 0.92). Some 400 or 1000 ppm of ethylenediaminetetraacetic acid (EDTA) was added to sequester calcium ions in the solution to avoid their inhibiting effect on nucleation.

For solutions with C:S-liq equal or less than 1:5, Na_2SO_4 was the dominant solid phase. For solutions with $1:5 < \text{C:S-liq} < 5:1$, burkeite was the dominant solid phase, with the Na_2CO_3 to Na_2SO_4 mole ratio in the solids increasing with increasing C:S-liq in solution. Also, the burkeite compositions in these experiments at 115 °C differed from the compositions expected by interpolating the previous equilibrium data at 100 °C and 150 °C. This was explained as the result of this study measuring crystal compositions that were controlled by kinetics rather than equilibrium.

For solutions with $5:1 < \text{C:S-liq} < 8:1$, a new double salt containing approximately 2 moles of Na_2CO_3 per mole of Na_2SO_4 was the dominant solid phase, with the Na_2CO_3 to Na_2SO_4 molar ratio in the solids increasing with increasing C:S-liq in solution (solution C:S-liq ratios of 5:1, 6:1, and 7:1 gave crystals with C:S ratios of 1.73, 1.91, and 2.2, respectively). This new species is termed "dicarbonate."

For solutions with C:S-liq equal or greater than 9:1, $\text{Na}_2\text{CO}_3\cdot\text{H}_2\text{O}$ was the dominant solid phase. The authors found it interesting that both the anhydrous and the monohydrate forms of Na_2CO_3 were crystallized from pure solutions, but the anhydrous form was absent when a small amount of Na_2SO_4 was present (e.g., at a C:S-liq ratio of 12:1). This was true even though the phase diagram shows the anhydrous form to be more stable at 115 °C (109 °C is the recognized transition temperature in the absence of sulfate). The authors concluded the most probable explanation was that crystallization was controlled by kinetics rather than by equilibrium, and the deciding factor was the relative nucleation and crystal growth rates of the stable and metastable phases. This behavior was generalized by Ostwald as “the rule of stages” (where an unstable system may transform into another transient state, whose formation involves the smallest loss of free energy, Mullin 2001).

The results of the single-crystal diffractometer study of synthetic burkeite (Guseppetti 1988) are used to discuss the unit cell and to rationalize the carbonate replacement of sulfate (concluding that the maximum C:S ratio is unity in burkeite). These earlier workers suggested that burkeite had no fixed formula and that the C:S ratio ranged from 1:3 to 1:2 (a range thought to be low because solutions with low C:S-liq ratios of 4:1 to 1:1 were used).

The XRD patterns of burkeite show shifting, intensity variation, and broadening of the lines as the C:S ratio changes. When the new species formed, there was no trace of the XRD patterns of burkeite or sodium carbonate (or its hydrates). The new species did match the XRD pattern reasonably well for a study described in a patent (Helvenston 1970), which was chemically analyzed to be a double salt with a C:S ratio of 2.25. Significant differences included the new species having peaks at 27.2° and 34.6°, and the absence of the burkeite peaks at 23.42°, 25.24°, and 31.93°.

3.2 Shi, B., Frederick, J. Jr., and R. W. Rousseau, 2003, “Nucleation Growth, and Composition of Crystals Obtained from Solutions of Na_2CO_3 and Na_2SO_4 ,” *Ind. Eng. Chem. Res.*, 42, 6343-47.

Formation of crystals from solutions containing Na_2CO_3 and Na_2SO_4 at 115°C is discussed. More details are provided, examples of which are now discussed. The effects of EDTA include producing crystals with higher carbonate content, and suppressing the varying amounts of $\text{Na}_2\text{CO}_3\cdot\text{H}_2\text{O}$ that formed at C:S-liq ratios below 9:1 (observed at 6:1 and 7:1). Details on the effects of scaling are discussed (no problem when burkeite forms, but severe scaling when calcium carbonate added, and different scaling problems when dicarbonate forms). Also, the paper discusses how the C:S ratio changes as the different crystals are formed, leading to three invariant points. An equation, fit to the data in the burkeite region, predicts the weight fraction of Na_2CO_3 in the solid from the fraction in the liquid. This leads to prediction of the conditions at the second nucleation point (where dicarbonate is produced).

One conclusion is that crystallization is greatly influenced by calcium. Calcium ions inhibit the nucleation of burkeite and the dicarbonate species, resulting in higher supersaturation and, in some cases, reversing the order of the nucleating species. Another conclusion is that scaling problems were encountered in two cases: (1) when calcium carbonate was added to solutions of high carbonate content in the burkeite region and (2) when the dicarbonate species crystallized.

3.3 Shi, B., Frederick, J. Jr., and R. W. Rousseau, 2003, "Effects of Calcium and Other Ionic Impurities on the Primary Nucleation of Burkeite," *Ind. Eng. Chem. Res.*, 42, 2861-69.

The primary nucleation of burkeite crystals from solutions containing Na_2CO_3 and Na_2SO_4 (with a C:S-liq molar ratio of 1:2) at 115 °C (usually) is discussed. Observations of unusual nucleation behavior led to explorations of which impurities affected nucleus formation. Calcium ions inhibit the nucleation of burkeite by substitution into the burkeite crystal lattice. A particle detector system was used to monitor primary and secondary nucleation, allowing division of the evaporative crystallization of burkeite into three regimes. The primary nucleation in regime I was found to result from the presence of 3 ppm to 5 ppm calcium ions in solution, which inhibited most primary nucleation. The growing burkeite crystals were found to concentrate the calcium, removing the calcium from solution. When the calcium ion concentration is reduced, primary nucleation of many small burkeite crystals occurs in the bulk solution during regime II.

As background information, the following items were presented. The most common industrial use of burkeite is in the detergent industry, where it has replaced phosphate carriers of detergent components. This study was prompted by the presence of burkeite in scale formed on heat-transfer surfaces in evaporators used to concentrate the black liquor used in the processing of wood pulp. Several things may contribute to scaling:

- a. Burkeite has the abnormal property of being less soluble at increased temperature (for the temperature range used); so the greatest supersaturation is at the higher temperatures of the heat-transfer surface. (However, this tendency was previously found to be unimportant at relatively low heating rates.)
- b. Burkeite crystals tend to act as agglomerating agents.
- c. Crystallization of burkeite is influenced by very small amounts of additives (e.g., phosphates and ionic polymers).

Nucleation can be either primary or secondary. The numbers of particles (of all sizes) showed a sudden onset as water was evaporated, which was from the primary nucleation. This was followed by a slower increase from a combination of secondary nucleation and crystal growth. When samples were taken for observation by an optical microscope, several large crystals were found to be present in regime I just before the onset of primary nucleation. The initial crystals grew very rapidly (some grew to over 500 μm) and were much larger than the small crystals formed after primary nucleation occurred. The results are interpreted to show that as water evaporates in regime I, it produces a few large crystals of burkeite by primary nucleation (these crystals have a C:S ratio of 1:2.7). In regime II, primary nucleation in the bulk solution produced a large number of very small crystals (these crystals have a C:S ratio of 1:2.25). In regime III, there was steady secondary nucleation and continued growth of burkeite crystals.

The inhibitive effect of the calcium ions is explained by the partial substitution of sodium ions in the lattice by calcium ions, which have nearly the same size but a different charge. This explanation is supported by results showing that two other ions (Ce^{3+} and Nd^{3+}) that have ionic radii within 5% of Na^+ also inhibit nucleation.

3.4 Shi, B., and R. W. Rousseau, 2001, "Crystal Properties and Nucleation Kinetics from Solutions of Na₂CO₃ and Na₂SO₄," *Ind. Eng. Chem. Res.*, **40**, 1541-47.

This paper discusses formation of crystals from solutions containing Na₂CO₃ and Na₂SO₄. The metastable zone widths for crystallization of Na₂CO₃ and burkeite were determined as functions of total solute concentration and the C:S molar ratio. Supersaturation was generated by increasing T at a constant rate.

Mullin (1993) reviews the classical theory of nucleation and expresses the rate of nucleation, J, as

$$J = A \exp [-G_{crit} / (k T)]$$

- J = number of nuclei formed per unit time per unit volume
 A = nucleation parameter (number per unit time per unit volume)
 G_{crit} = free energy change to form a stable nucleus (J/mol)
 k = Boltzmann constant (1.38 x 10⁻²³ J/mol/K)
 T = temperature (K).

The solubilities and the metastable limits (at different heating rates) for crystallization of Na₂CO₃ (anhydrous and monohydrate) and burkeite were determined at T values from 100 °C to 170 °C. Their measurements used the crystallizing method, while previous workers used the dissolving method. Comparison of the two methods found the dissolving method to give a higher solubility, by about 4%. The solubility measurements and those of previous workers (except for the burkeite values by Makarov and Krasinkov, cited in Linke 1965) were correlated by ignoring the weak temperature dependence on the solution density in an approximation to ideal solution theory to give the solubility as

$$\ln(w^*) = C_1 / T + C_2$$

- w* = mass fraction at equilibrium
 C₁, C₂ = parameters (C₁ is proportional to the heat of fusion)

The similarity of the shapes of the solubilities and metastable limits suggested expressing the solubility limits as

$$\ln(w) = C_1 / T_{nuc} + C_2$$

- w = mass fraction of metastable limit
 T_{nuc} = nucleation temperature

These two equations are used to estimate the supersaturation at nucleation. Table 3.1 shows the fitted parameters for solubilities and metastable limits (the metastable limits are shown for one heating rate).

Table 3.1. Correlation Parameters for Solubilities and Metastable Limits.

System	Type of Data	C ₁	C ₂
Na ₂ CO ₃ —H ₂ O	Solubility	499.94	-2.476
Na ₂ CO ₃ —H ₂ O	Metastable, 0.6 K/min	497.12	-2.4166
Burkeite—H ₂ O	Solubility	362.68	-2.2346
Burkeite—H ₂ O	Metastable, 0.6 K/min	404.27	-2.1981

The addition of 5 wt % of NaOH lowered the solubility of burkeite and significantly reduced the metastable limits (reducing the metastable zone width by 30%).

The critical cluster size for Na₂CO₃ was estimated as 8 nm to 10 nm, which was consistent with the ranges found for different system by earlier workers (0.78 to 4.32, 3.1 to 9.8, and 2 to 4 nm).

The burkeite crystals initially had a C:S ratio of 1:2.2; aging the crystals at 120 °C changed the ratio at longer aging times, reaching a ratio of 1:2.07 after 48 hr (close to the nominal ratio of 1:2.0).

4. SOLUBILITIES AND OTHER TOPICS

Data on the solubilities are tabulated in the two volumes of Linke (1965). However, it is interesting to see a table comparing the solubilities of various sodium compounds. Such a table is given in http://chemdat.merck.de/cdrl/services/labtools/en/table_solinr.html and an excerpt is reproduced in Table 4.1.

4.1 Xu, T., and K. Pruess, 2001, *Thermophysical Properties of Sodium Nitrate and Sodium Chloride Solutions and Their Effects on Fluid Flow in Unsaturated Media*, LBNL-48913, Lawrence Berkeley National Laboratory, Berkeley, CA.

The purpose of this study is to contribute a basic understanding of effects of the thermophysical behavior of NaNO₃ solutions on fluid flow in unsaturated media. The study first presents mathematical expressions for the dependence of density, viscosity, solubility, and vapor pressure of NaNO₃ solutions on both salt concentration and temperature, which were determined by fitting from published measured data. The thermophysical behavior of sodium chloride solutions are also given for comparison. The functional thermophysical properties are implemented into a new TOUGH2 equation-of-state module. This simulation tool is used to investigate effects of the thermophysical properties on fluid flow in unsaturated media, focusing on the effect of vapor pressure lowering due to salinity. Simulations are given of a one-dimensional problem to study this salinity-driven fluid flow. A number of simulations were performed using different values of thermal conductivity, permeability, and temperature, to illustrate conditions and parameters controlling these processes.

Table 4.1. Solubilities of Sodium Compounds.

Formula	Solubility in g/100 g H ₂ O at °C						Solution Density at 20 °C
	0	20	40	60	80	100	
NaCH ₃ COO·3H ₂ O	36.3	46.4	65.4	138.0 (58°C)	-	-	1.17
NaBr	-	-	-	118.0	118.3	121.2	-
Na ₂ CO ₃ ·10H ₂ O	6.86	21.7	-	-	-	-	1.1941
Na ₂ CO ₃ ·H ₂ O	-	-	48.9	46.2	44.5	44.5	-
Na ₂ CO ₃	7.1	21.4	48.5	46.5	45.8	45.5	-
NaCl	-	35.9	36.4	37.1	38.1	39.2	1.201
Na ₂ CrO ₄	-	-	-	-	124.0	125.9	-
Na ₂ Cr ₂ O ₇ ·2H ₂ O	163.2	180.2	220.5	283.0	385.0	-	-
NaH ₂ PO ₄ ·2H ₂ O	57.7	85.2	138.2	-	-	-	-
NaH ₂ PO ₄	-	-	-	179.3	207.3	284.4	-
Na ₄ P ₂ O ₇ ·10H ₂ O	2.7	5.5	12.5	21.9	30.0	40.3	1.05
Na ₂ S ₂ O ₅	-	65.3	71.1	79.9	88.7	(100.0)	-
NaF	(3.6)	4.1	-	-	-	-	1.04
NaHCO ₃	6.89	9.6	12.7	16.0	19.7	23.6	1.08
Na ₂ HPO ₄ ·12H ₂ O	1.63	7.7	-	-	-	-	1.08
Na ₂ HPO ₄ ·7H ₂ O	-	-	55.0	-	-	-	-
Na ₂ HPO ₄ ·2H ₂ O	-	-	-	83.0	92.4	-	-
Na ₂ HPO ₄	-	-	-	-	-	104.1	-
NaOH·H ₂ O	-	109.2	126.0	178.0	-	-	1.55
NaOH	-	-	-	-	313.7	341.0	-
NaIO ₃	2.5	9.1	-	23.0	27.0	32.8	-
NaI	-	-	-	-	295.0	303.0	-
NaNO ₃	70.7	88.3	104.9	124.7	148.0	176.0	1.38
NaNO ₂	73.0	84.5	95.7	112.3	135.5	163.0	1.33
NaClO ₄ ·H ₂ O	167.0	181.0	243.0	-	-	-	1.757
Na ₃ PO ₄ ·12H ₂ O	1.5	12.1	31.0	55.0	81.0	108.0	1.106
Na ₂ SO ₄ ·10H ₂ O	4.56	19.2	-	-	-	-	1.150
Na ₂ SO ₄	-	-	48.1	45.3	43.1	42.3	-
Na ₂ S·9H ₂ O	12.4	18.8	29.0	-	-	-	1.18
Na ₂ SO ₃	-	-	37.0	33.2	29.0	26.6	-
Na ₂ B ₄ O ₇	1.2	2.7	6.0	20.3	31.5	52.5	-
Na ₂ S ₂ O ₃ ·5H ₂ O	52.5	70.1	102.6	-	-	-	1.39

Results indicate that heat conduction plays a very important role in this salinity-driven vapor diffusion by maintaining a nearly constant temperature. The smaller the permeability, the more water is transferred into the saline environment. Effects of permeability on water flow are also complicated by effects of capillary pressure and tortuosity. The higher the temperature, the more significant the salinity driven fluid flow.

4.2 Hill, C. A., 1981, "Mineralogy of Cave Nitrates," *The NSS Bulletin*, **43**, 127-32.

Nitrate minerals occur in dry southwestern U.S. caves but do not crystallize in humid southeastern caves. At 12 °C, the humidity at which nitrate minerals crystallize is 54% for nitrocalcite [$\text{Ca}(\text{NO}_3)_2 \cdot 4\text{H}_2\text{O}$] and nitromagnesite [$\text{Mg}(\text{NO}_3)_2 \cdot 6\text{H}_2\text{O}$], 74% for ammonia-niter (NH_4NO_3), 79% for soda-niter (NaNO_3), and 92% for niter (KNO_3).

The nitrate minerals niter, soda-niter, and darapskite [$\text{Na}_3(\text{NO}_3)(\text{SO}_4) \cdot \text{H}_2\text{O}$] have been identified in non-salt peter, southwestern caves. Niter (crystal size = 1.5 mm) occurs as a transparent, colorless to light brown, bitter-tasting wall crust in a lava tube near Socorro, New Mexico. Soda-niter also occurs as a crystalline wall crust, as two small stalactites, and as one small stalagmite with the Socorro niter. The Socorro soda-niter crystals are rhombohedral, 2 to 3 mm long, transparent, and colorless. Darapskite occurs in Flower Cave, Big Bend National Park, Texas, as cave "flowers," crust, "hair," flowstone, and stalactites. The darapskite is colorless with $2V(-) = 20\text{-}30^\circ$, $\alpha = 1.30 \pm 0.005$, $\beta = 1.480 \pm 0.003$, $\gamma = 1.489 \pm 0.003$, $a = 10.558(3)$, $b = 6.870(2)$, $c = 5.186(1)$ and $\beta = 101.46.1(5)$.

5. COMPARISONS WITH THERMODYNAMIC CALCULATIONS

This section describes results from the <http://www.phasediagram.dk> website that show calculations by Kaj Thomsen from his thesis and publications with coworkers (Thomsen 1997 and other Thomsen references, whose abstracts appear at the end of this section).

The model used is the Extended UNIQUAC model, which is a thermodynamic model applicable to aqueous solutions of electrolytes and nonelectrolytes. The model describes the phase behavior and the thermal properties of electrolyte solutions. The accuracy of solid-liquid equilibrium calculations is usually within ± 1 wt %. The temperature range for the model parameters used here is from about -50 °C to 110 °C.

5.1 NaNO_3 - Na_2SO_4 - H_2O System

5.1.1 Ternary Phase Diagram

Figure 5.1 shows a ternary phase diagram for the NaNO_3 - Na_2SO_4 - H_2O system in the temperature range from -20 °C to 110 °C. The equilibrium compositions were calculated using the Extended UNIQUAC model. Experimental points from several different investigators are marked in the same diagram to illustrate the quality of the fit. All points in the diagram represent saturated solutions, as Figure 5.1 is plotted as a temperature/two-salt saturation point diagram. The lines in the diagram represent compositions where two salts are in equilibrium with the same liquid (and with a gas phase). The line intersections represent compositions at which three solid salts are in equilibrium with the same liquid (and with a gas phase). These points are invariant points.

The solid phases encountered in this system in the temperature range from -20 °C to 110 °C are the following.

- Ice, $\text{Na}_2\text{SO}_4 \cdot 10\text{H}_2\text{O}$ (Glauber salt).
- Na_2SO_4 (sodium sulfate).
- $\text{NaNO}_3 \cdot \text{Na}_2\text{SO}_4 \cdot \text{H}_2\text{O}$ (darapskite).
- NaNO_3 (sodium nitrate).

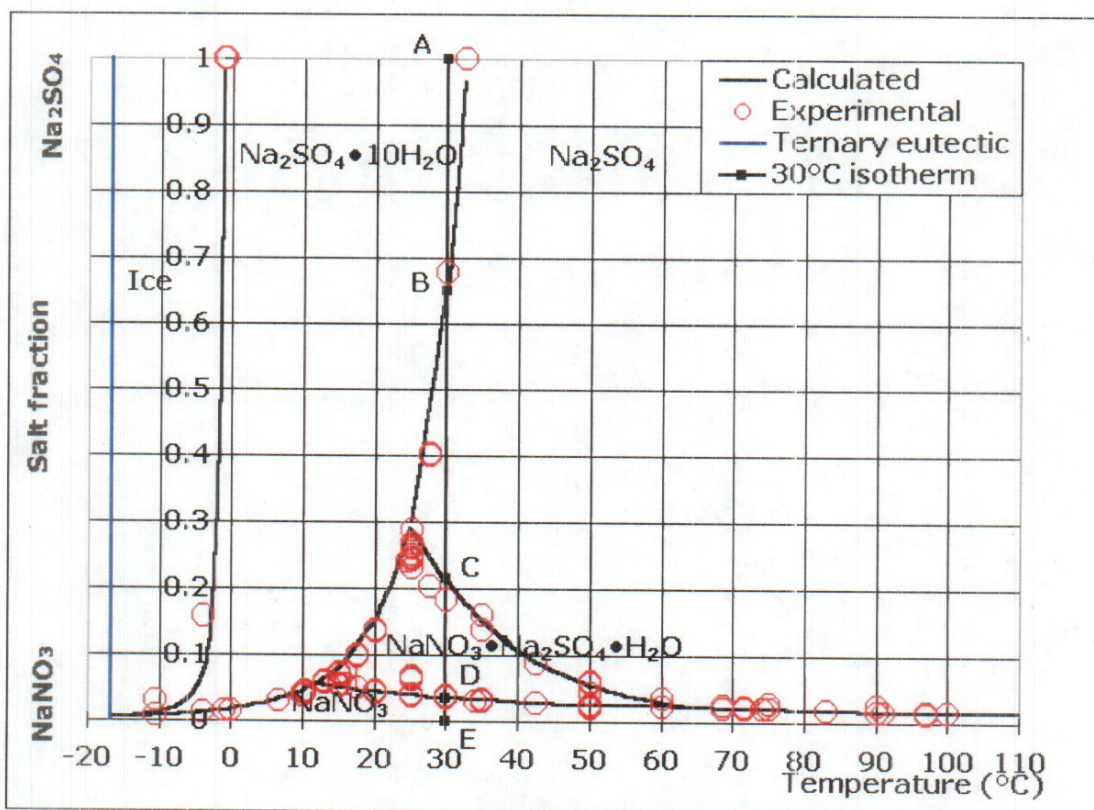


Figure 5.1. Ternary Phase Diagram for the NaNO_3 - Na_2SO_4 - H_2O System.

The vertical line at the left marks the lowest temperature at which an aqueous solution can be in equilibrium with ice and salts in this ternary system. At temperatures lower than this, an equilibrium mixture of water and the two salts will consist of the three separate phases: $\text{Na}_2\text{SO}_4 \cdot 10\text{H}_2\text{O}$ (Glauber salt), NaNO_3 (sodium nitrate), and ice.

The ordinate in Figure 5.1 is "salt fraction," moles of Na_2SO_4 divided by (mol Na_2SO_4 + mol NaNO_3). [However, the curves look the same as in similar diagrams in Thomsen (1997) and Thomsen, Rasmussen, and Gani (1998) where "salt fraction," is defined on an equivalent basis as twice the molality of Na_2SO_4 divided by (twice the molality of Na_2SO_4 + molality of NaNO_3).] The points in the diagram therefore mark compositions on a dry basis. The corresponding water content is not marked, but it could be marked as a third dimension. Alternatively, solubility isotherms could be calculated. The temperature is held constant, and all concentrations can be shown in two dimensions.

5.1.2 Solubility Isotherm at 30°C

The 30 °C solubility isotherm is shown in Figure 5.2. The solubility isotherm calculated with the Extended UNIQUAC model is shown together with experimental data. The solubility isotherm is marked with the letters A, B, C, D, E, corresponding to the points marked with the same letters in Figure 5.1. The concentration unit in Figure 5.2 is weight percent. The green lines in the diagram are tie lines, marking the borders of fields yielding a certain solid salt.

- a. The solubility line from A to B marks solutions in equilibrium with Glauber salt. A mixture with a gross composition in the field marked I will at equilibrium yield solid Glauber salt and a saturated liquid on AB.
- b. The solubility line from B to C marks solutions in equilibrium with anhydrous sodium sulfate. A mixture with a gross composition in the field marked II will at equilibrium yield solid anhydrous sodium sulfate and a saturated liquid on BC.
- c. The line CD marks saturated solutions in equilibrium with darapskite.
- d. The line DE marks saturated solutions in equilibrium with sodium nitrate.
- e. A solution with a gross composition in the field marked V will at equilibrium yield a saturated liquid of composition B and the two solid phases: Glauber salt and anhydrous sodium sulfate.
- f. A solution with a gross composition in the field marked VI will at equilibrium yield a saturated liquid of composition C and the two solid phases: anhydrous sodium sulfate and darapskite.
- g. A solution with a gross composition in the field marked VII will at equilibrium yield a saturated liquid of composition D and the two solid phases: darapskite and sodium nitrate.

5.2 Flowsheet Application Examples

5.2.1 Simulation and Optimization of Potassium Nitrate Production

Ullmann, 1991, mentions a process employed in Chile for the production of potassium nitrate from potassium chloride and sodium nitrate. The potassium chloride is produced from the Atacama Salar brines by evaporation in solar ponds and subsequent separation from sodium chloride by a grinding and flotation process. Sodium nitrate is produced by leaching crushed caliche ore and cooling the solution.

Two alternative flowsheet designs of this fractional crystallization process were made with a process synthesis program (Thomsen et al. 1995). Both flowsheet designs were then optimized with the simulation program to maximize the yield of KNO_3 . The design variables were the

amount of water added to the system, the percentage of water evaporated in the NaCl crystallizer, and the percentage of the recirculation stream removed (purged).

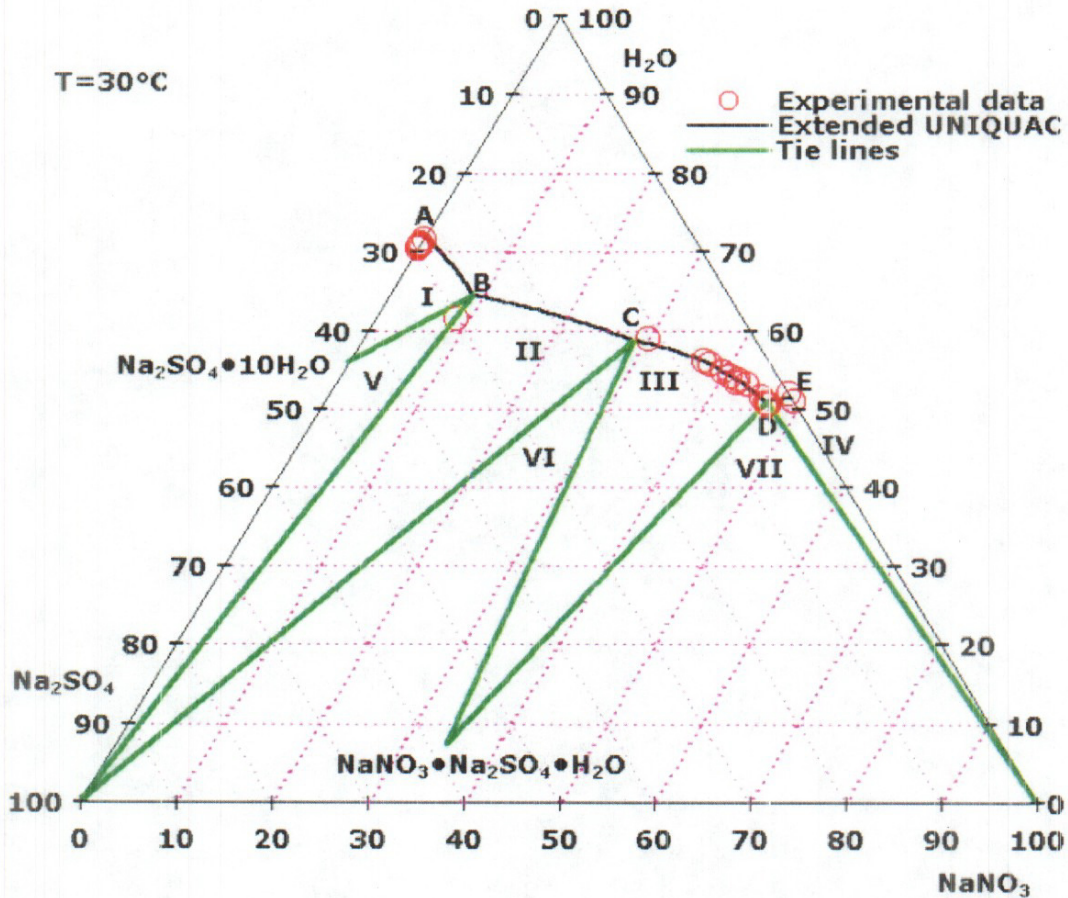


Figure 5.2. Solubility Isotherm at 30°C for the NaNO₃-Na₂SO₄-H₂O System.

Figure 5.3 displays one of the designs (design one). The yield of potassium nitrate is approximately the same in the two designs, but the energy consumption for heating and cooling is significantly different. Design one requires about twice as much heating (11867 kJ/h as opposed to 5201 kJ/h) but only about half as much cooling (1392 kJ/h as opposed to 3066 kJ/h). Furthermore, the size of the recirculation stream in design one is less than half of the recirculation stream in design two. If the evaporation is performed in solar evaporation ponds as indicated, the heat consumption may be of minor importance, so that design one would be the most efficient.

Caliche ore contains sodium sulfate. The raw material for the KNO₃ production may therefore also contain some sodium sulfate. Figure 5.4 shows what effect a small content of sodium sulfate will have on design one. The flowsheet was optimized for the maximum yield of KNO₃.

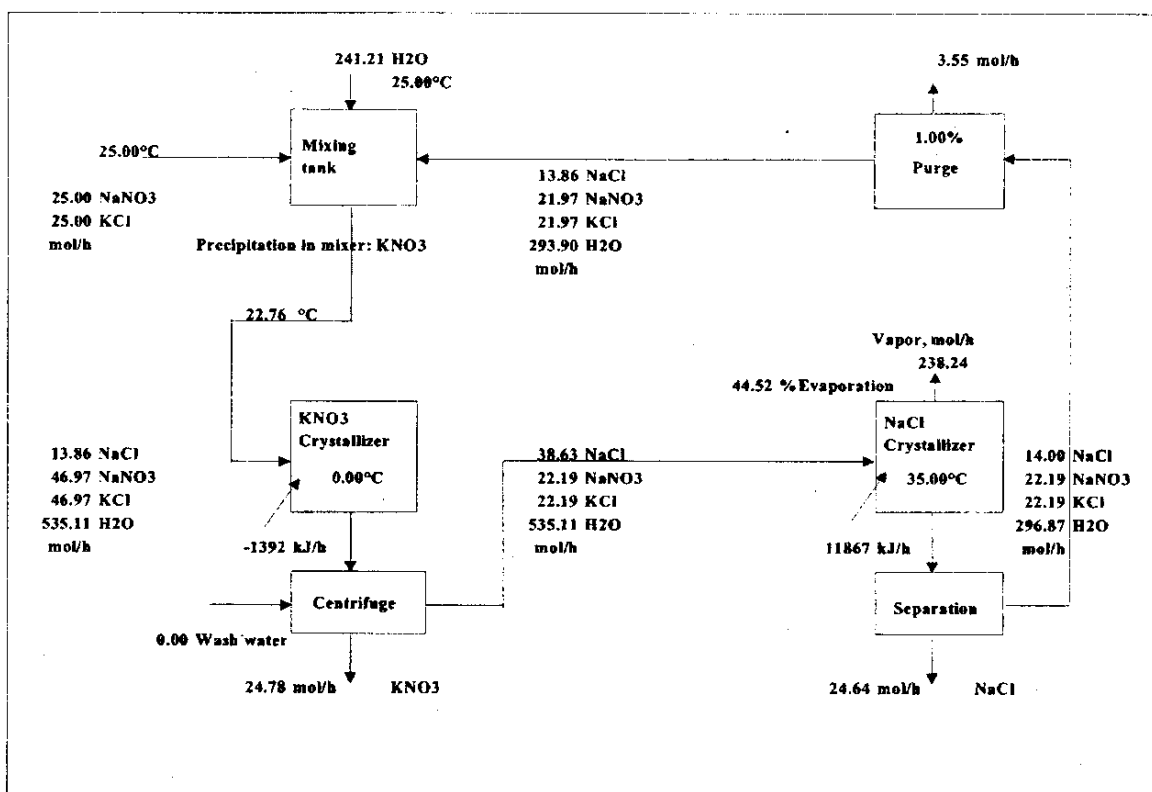


Figure 5.3. Production of KNO_3 from NaNO_3 and KCl , Design One.

As it appears from Figure 5.4, the same yield of KNO_3 can be obtained as in the system without Na_2SO_4 . KNO_3 , however, is the only pure product obtained from the process. A complete separation of the feed into three pure products would require an additional crystallization process. If a feed containing Na_2SO_4 was used in connection with design two (1) the amount of water added between the two crystallizers would be about 10 times as large as the amount used in the absence of Na_2SO_4 , (2) the recirculation stream would become larger, and (3) the amount of heat required for evaporating water would grow considerably. Thus, design one is clearly the most advantageous if the feed contains Na_2SO_4 .

5.2.2 Simulation/Optimization of K_2SO_4 Production Process

A patented process (Sogolov et al. 1982; Neitzel 1986) for the production of K_2SO_4 and NaCl from Na_2SO_4 and KCl was simulated and improved through optimization. The mass balance given in the patent description (Sogolov et al. 1982) is incomplete, and the temperature of the sodium chloride crystallizer is not given.

An open loop simulation (i.e., the stream supposed to be recycled is purged) of the process was performed with the simulation program (Figure 5.5). The four solid product streams from the four crystallizers were fitted to $<1\%$ deviation by weight compared to the data given in the patent description. The temperature of the sodium chloride crystallizer and the stream variables of the recirculation stream were used as design variables.

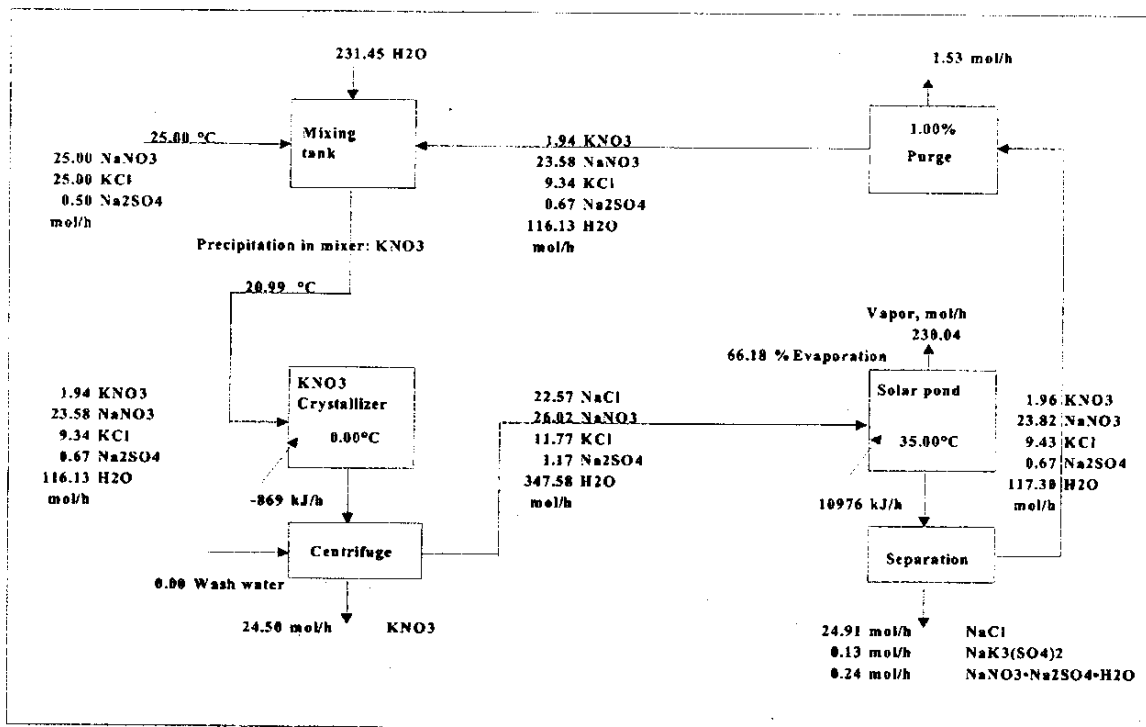


Figure 5.4. Production of KNO_3 from $NaNO_3$ and KCl containing Na_2SO_4 , Design One.

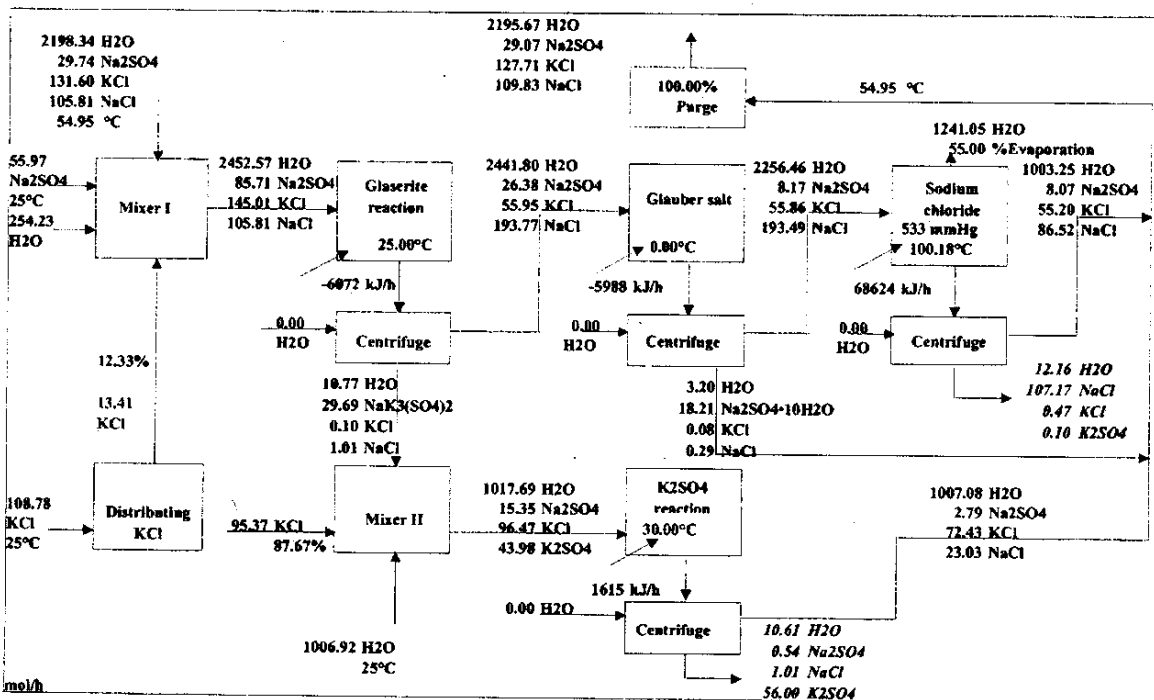


Figure 5.5. Open Loop Simulation of Production of K_2SO_4 + $NaCl$ from Na_2SO_4 + KCl .

Note: The boxes marked Glaserite reaction, Glauber salt, Sodium chloride, and K_2SO_4 reaction represent crystallizers.

In all crystallizers the entrainment of mother liquor with the crystals was set to 7.5%. This percentage gives the moles of mother liquor per mole of ions in the crystals. A 7.5 mol% entrainment of mother liquor will typically mean 2% to 5% by weight, depending on the salt. The resulting recirculation stream falls within the boundaries given in the patent description.

The main disadvantage of this process is the large amount of heat needed to evaporate water in the sodium chloride crystallizer. According to the patent description, more than 2.23 kg water is evaporated for each kilogram of K_2SO_4 produced.

The process was optimized with the simulation program. The objective of the optimization was to find the process parameters yielding products of the same purity as described in the patent but with the lowest possible amount of heat exchanged between or added to the four crystallizers. In the optimized process, only 1.88 kg water needs to be evaporated for each kilogram of K_2SO_4 produced. Thus, approximately 84% of the amount evaporated in the patented process is needed in the optimal solution.

The most significant result of the optimization is that no water needs to be added to Mixer I, which reduces the amount of water to be evaporated by about 16%. The amount of heat exchanged between or added to the crystallizers is reduced by more than 25%. Also the size of the recirculation stream is reduced by about 20%. The temperatures of the sodium chloride and the K_2SO_4 reaction crystallizers can be increased, for example, to 111 °C and 30 °C, respectively, without altering these facts.

5.3 Abstracts of Selected Thomsen Publications

The following abstracts describe details on the thermodynamic model and several examples of applications of the model by Thomsen and his coworkers.

Christensen, S. G., and K. Thomsen, 2003, "Modeling of Vapor-Liquid-Solid Equilibria in Acidic Aqueous Solutions," *Ind. Eng. Chem. Res.* 42, 4260-4268.

The phase behavior [vapor-liquid equilibria (VLE) and solid-liquid equilibria (SLE)] and thermal properties of aqueous solutions of ions (e.g., K^+ , Na^+ , NH_4^+ , Ca^{2+} , Cl^-) in the presence of phosphoric acid and nitric acid are described by means of the Extended UNIQUAC model. Model parameters are evaluated on the basis of more than 2000 experimental data points. There is good agreement between calculated and experimental data points. The model parameters are valid in the temperature range from -18 °C to 122 °C and in the concentration range up to 12 molal for the acids HNO_3 and H_3PO_4 .

Iliuta, M. C., K. Thomsen, and P. Rasmussen, 2002, "Modeling of Heavy Metal Salt Solubility Using the Extended UNIQUAC Model," *AIChE J.*, 48, 2664-2689.

Solid-liquid equilibria in complex systems involving a heavy metal cation (Mn^{2+} , Fe^{2+} , Co^{2+} , Ni^{2+} , Cu^{2+} , or Zn^{2+}) and one or more ions for which Extended UNIQUAC parameters have been published previously are modeled using the Extended UNIQUAC model. Model parameters are

determined on the basis of a databank with more than 4000 experimental data points for binary and ternary systems. The parameters are generally valid in the temperature range from the cryohydratic point to the boiling point of the respective solutions.

Iliuta, M., K. Thomsen and P. Rasmussen, 2000, "Extended UNIQUAC Model for Correlation and Prediction of Vapour-Liquid-Solid Equilibria in Aqueous Salt Systems Containing Non-Electrolytes. Part A. Methanol-Water-Salt systems," *Chem. Eng. Sci.*, 55, 2673-2686.

The Extended UNIQUAC model has previously been used to describe the excess Gibbs energy for aqueous electrolyte mixtures. It is an electrolyte model formed by combining the original UNIQUAC model, the Debye-Hückel law, and the Soave-Redlich-Kwong equation of state. In this work the model is extended to aqueous salt systems containing nonelectrolytes to demonstrate its ability in representing solid-liquid-vapour (SLV) equilibrium and thermal property data for these strongly non-ideal systems. The model requires only pure component and binary temperature dependent interaction parameters. The calculations are based on an extensive database consisting of salt solubility data in pure and mixed solvents, VLE data for solvent mixtures and mixed solvent-electrolyte systems and thermal properties for mixed solvent solutions. Application of the model to the methanol-water system in the presence of several ions (Na^+ , K^+ , NH_4^+ , Cl^- , NO_3^- , SO_4^{2-} , CO_3^{2-} , and HCO_3^-) shows that the Extended UNIQUAC model is able to give an accurate description of VLE and SLE in ternary and quaternary mixtures, using the same set of binary interaction parameters. The capability of the model to predict accurately the phase behavior of methanol-water-three salts systems is illustrated.

Thomsen, K., and P. Rasmussen, 1999, "Modeling of Vapor-Liquid-Solid Equilibria in Gas-Aqueous Electrolyte Systems," *Chem. Eng. Sci.* 54, 1787-1802.

A thermodynamic model for the description of vapor-liquid-solid equilibria is introduced. This model is a combination of the extended UNIQUAC model for electrolytes and the Soave-Redlich-Kwong cubic equation of state. The model has been applied to aqueous systems containing ammonia and/or carbon dioxide along with various salts. Model parameters valid in the temperature range 0-110 °C, the pressure range from 0-100 bar, and the concentration range up to approximately 80 molal ammonia are given. The model parameters were evaluated on the basis of more than 7000 experimental data points.

Thomsen, K., P. Rasmussen, and R. Gani, 1998, "Simulation and Optimization of Fractional Crystallization Processes," *Chem. Eng. Sci.*, 53, 1551-1564.

A general method for the calculation of various types of phase diagrams for aqueous electrolyte mixtures is outlined. It is shown how the thermodynamic equilibrium precipitation process can be used to satisfy the operational needs of industrial crystallizer/centrifuge units. Examples of simulation and optimization of fractional crystallization processes are shown. In one of these examples a process with multiple steady states is analyzed. The thermodynamic model applied for describing the highly non-ideal aqueous electrolyte systems is the Extended UNIQUAC model.

Thomsen, K., 1997, "Aqueous Electrolytes: Model Parameters and Process Simulation," Ph.D. thesis, Department of Chemical Engineering, Technical University of Denmark.

This thesis deals with aqueous electrolyte mixtures. The Extended UNIQUAC model is used to describe the excess Gibbs energy of such solutions. Extended UNIQUAC parameters for the 12 ions (Na^+ , K^+ , NH_4^+ , H^+ , Cl^- , NO_3^- , SO_4^{2-} , HSO_4^- , OH^- , CO_3^{2-} , HCO_3^- , and $\text{S}_2\text{O}_8^{2-}$) are estimated. A computer program including a steady-state process simulator for the design, simulation, and optimization of fractional crystallization processes is presented.

Thomsen, K., P. Rasmussen, and R. Gani, 1996, "Correlation and Prediction of Thermal Properties and Phase Behaviour for a Class of Aqueous Electrolyte Systems," *Chem. Eng. Sci.*, 51, 3675-3683.

An extended UNIQUAC model is used to describe phase behavior (VLE, SLE) and thermal properties (heat of mixing, heat capacity) for aqueous solutions containing ions [e.g. (Na^+ , K^+ , H^+) (Cl^- , NO_3^- , SO_4^{2-} , OH^- , CO_3^{2-} , HCO_3^-)]. A linear temperature dependence of the binary interaction parameters allows good agreement with experimental data in the temperature range 0 °C-110 °C.

Thomsen, K., R. Gani, and P. Rasmussen 1995, "Synthesis and Analysis of Processes with Electrolyte Mixtures," *Computers and Chemical Engineering*, 19S, S27-S32.

A computer-aided system for synthesis, design, and simulation of crystallization and fractional crystallization processes with electrolyte mixtures is presented. The synthesis methodology is based on the use of computed solubility diagrams for the corresponding electrolyte systems. For a specified crystallizer and product(s), the process flowsheet along with conditions of operation is determined, while for a specified feed mixture and product(s), the process flowsheet together with the type of crystallizer is determined. To verify the "determined" flowsheet an option to perform steady-state simulation is also provided. Examples highlighting the various features of the computer-aided system are presented.

6. CRYSTALLIZATION SYSTEMS AND CRYSTALLIZERS

Many suppliers of crystallization systems and crystallizers are found on the internet. Examples of information are presented in the following. As a point of reference to the Hanford site, the 242-A Evaporator/Crystallizer is a forced circulation, vacuum evaporator/crystallizer.

6.1 Swenson Technology, Inc.

26000 Whiting Way, Monee Illinois 60449-8060
708-587-2300, <http://www.swensontechnology.com>

Swenson Technology is an industry recognized leader in process equipment. Equipment to meet processing needs can be supplied world-wide. They specialize in equipment used in the chemical, pharmaceutical, and waste reduction industries to convert liquid solutions into dry

solids. Swenson can supply equipment for erection by the purchaser, skid mounted, or in complete turn-key installations.

Swenson has an unusually broad background in the crystallization field, which includes manufacture of sugar crystallizers in the latter part of the 19th century, crystallizing calandria evaporators in the early 1900s, introduction of the Swenson-Walker surface-cooled crystallizer in the 1920s, patents on and development of the first low-temperature vacuum crystallizer in the 1930s, and extensive development of the forced-circulation evaporative crystallizer in the 1950s. The number of vacuum crystallizer applications alone exceeds 350.

The SWENSON Draft Tube Baffle (DTB) crystallizer is the newest and the most successful of the crystallizers designed to make the large, uniform crystals required for fertilizer and similar applications where superior filtration, centrifugation, washing, drying, and storage characteristics are required. This machine is the result of years of research and development as well as proven plant scale operation in more than 300 installations.

They have test facilities with pilot-plant-sized vacuum-cooled, forced-circulation, and DTB crystallizers, where solutions may be tested, the results compared, and the best design offered for the required product characteristics.

Swenson crystallizers have performed successfully in a number of industrial applications. A partial list of materials that have been processed in Swenson crystallizers follows:

- Ammonium bifluoride
- Ammonium chloride
- Ammonium sulfate
- Anhydrous sodium thiosulfate
- Barium chloride dihydrate
- Calcium sucaryl
- Citric acid
- Diammonium phosphate
- Dimethylterephthalate
- Glutamic acid
- Hydroquinone
- Lithium carbonate
- Lithium chloride
- Monosodium glutamate
- Oxalic acid
- Potassium chloride
- Potassium nitrate
- Potassium permanganate
- Monopotassium phosphate
- Silver nitrate
- Sodium bichromate and sodium chromate
- Sodium bromide
- Sodium carbonate
- Sodium chlorate
- Sodium chloride
- Sodium citrate dihydrate
- Sodium ferrocyanide
- Sodium sucaryl
- Sodium Sulfate
- Sodium sulfite
- Sodium thiosulfate
- Sugar
- Sulfamic acid
- Trisodium phosphate
- Urea

6.1.1 Surface-Cooled Crystallizers (Low Temperature/High Boiling Point Elevation)

For operation at temperatures below which it is not economically feasible to use vacuum equipment, or for solutions with very high boiling point elevations, the SWENSON Surface-Cooled Crystallizer is generally specified.

The surface-cooled unit is a type of forced-circulation crystallizer consisting of a shell and tube heat exchanger through which is pumped the slurry of growing crystals, a crystallizer body to provide retention time, and a recirculation pump and piping. Within the crystallizer body is a baffle designed to keep excessively fine crystals separated from the growing magma for size and slurry density control purposes.

The circulation rate through the heat exchanger is normally high enough so the temperature drop is in the range of 1 °F-2 °F. Surrounding the tubes is the cooling media—either tempered water circulated through segmented baffles or a vaporized refrigerant.

Because the tube wall is the coldest part of the crystallizing system, the temperature differences between the wall and the slurry being pumped through the tube must be as small as practical. Practical values depend on the operating cycles and the properties and characteristics of the materials. Temperature differences ranging from 5 °F to 15 °F are required to achieve reasonable operating cycles.

Surface-cooled crystallizers are used where the solution's boiling point elevation is extremely high, as in the case of caustic solutions, or when the temperature level is so low evaporation by vacuum is impossible. Typical applications for the SWENSON Surface-Cooled Crystallizer are in processing sodium chloride from caustic solutions, sodium carbonate decahydrate from waste solutions, and sodium chlorate from solutions saturated with sodium chloride.

6.1.2 Forced-Circulation Crystallizer

6.1.2.1 High Evaporation Rates

For feeds where high rates of evaporation are required, where there are scaling components, or when crystallization must be achieved in solutions with inverted solubility or relatively high viscosity, the SWENSON Forced-Circulation Crystallizer is the best choice.

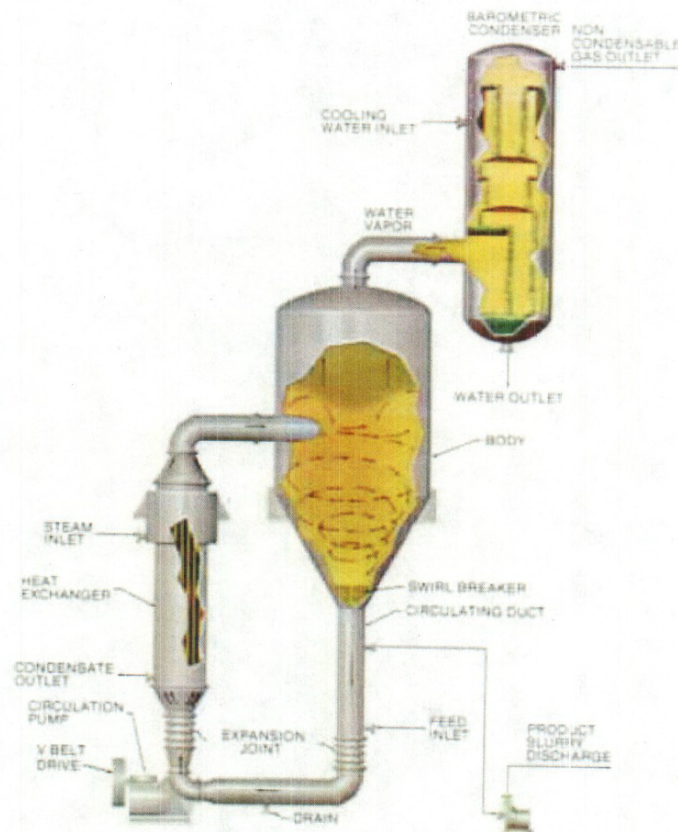
This type of unit—also known as the circulating magma crystallizer or the mixed suspension-mixed product removal (MSMPR) crystallizer—consists of a body sized for vapor release with a liquid level high enough to enclose the growing crystals. Suction from the lower portion of the body passes through a circulation pump and a heat exchanger and returns to the body through a tangent or vertical inlet. The heat exchanger is omitted when adiabatic cooling is sufficient to produce a yield of crystals. See Figure 6.1.

The most common use of this crystallizer is as an evaporative crystallizer with materials having relatively flat or inverted solubility. It is also useful with compounds crystallized from solutions with scaling components.

6.1.2.2 Controlled Supersaturation

When the heat exchanger is used, it is normally one- or two-pass and is designed for relatively low temperature rises in the solution. This limits the supersaturation of scaling components when heating materials of inverted solubility. In most applications, the steam-to-liquid, delta-T is also limited to prevent mass boiling within the tubes or vaporization at the tube wall.

Figure 6.1. SWENSON Forced-Circulation Crystallizer.



6.1.2.3 Most Widely Used Crystallization Method

Forced circulation is the most widely practiced method of crystallization. Forced-circulation crystallizers are found in sizes ranging from 2-ft diameter laboratory models to over 40-ft diameter units for continuous processing. Per pound of product, it is ordinarily the most inexpensive type of equipment available, particularly when substantial amounts of evaporation are required.

SWENSON Forced-Circulation Crystallizers can be operated on a batch basis but their most frequent use is for continuous processing of such materials as sodium chloride, sodium sulfate,

sodium carbonate monohydrate, citric acid, monosodium glutamate, urea, and similar crystalline materials.

6.1.2.4 Recompression Crystallization

For applications where the solution's boiling point elevation is low, such as for sodium carbonate, it is possible to significantly reduce the cost of the operation by vapor recompression. In this technique the vapor, which is removed to precipitate the crystalline product, is compressed by a positive displacement or centrifugal compressor to a pressure high enough so that it may be used as steam in the heat exchanger.

By proper heat exchange, many mechanical recompression applications can operate efficiently without any external source of heat, except for startup purposes. For other applications, a small quantity of steam is required at the heating element to maintain the system on a continuous basis.

The drive for the compressor may be either a steam turbine or an electric motor depending on the availability and cost of power. To minimize power requirements, the heat exchanger is designed for the lowest possible delta-T, thereby minimizing salting and scaling.

A steam booster can be used in lieu of a mechanical compressor when steam costs are relatively inexpensive compared to electrical power costs. In this case, part of the vapor is compressed by the high-pressure steam in the booster and used as the first-effect heating media. Vapor not compressed goes to the second effect. The recompression crystallization technique can also be applied to the DTB or SWENSON OSLO (growth type) crystallizers.

6.1.3 **Draft Tube Baffle Crystallizer**

6.1.3.1 Superior Control Over Crystal Size and Characteristics

For superior control over particle size when excessive fine crystals are present, the SWENSON Draft Tube Baffle (DTB) crystallizer has proven highly effective. This type of crystallizer is used primarily in the production of a variety of large-size crystalline materials such as ammonium sulfate, potassium chloride, and diammonium phosphate for the fertilizer industry.

The DTB crystallizer is built in both the adiabatic cooling and evaporative types and consists of a body in which growing crystals are circulated from the lower portion to the boiling surface by means of a large, slow-moving propeller circulator. Surrounding the suspended magma is an annular settling zone from which a stream of mother liquor bearing fine crystals can be removed. These fines are separated from the growing suspension of crystals by gravitational settling in the annular baffle zone.

Fines leaving the baffle zone are sent to a following stage, settler, or heat exchanger in the case of an evaporative DTB crystallizer. The mother liquor is returned to the suction of the propeller circulator after the fines have been destroyed by heating or mixing with dilute feed or water, depending on the flowsheet.

6.1.3.2 Low Temperature Rise at Low Power Input

In the case of adiabatic cooling or evaporative crystallizers, the temperature rise in the circulated magma caused by the mixing of the incoming feed or heated mother liquor at the eye of the propeller is approximately 1°F and thereby limits the supersaturation rate to very low values. The boiling action is concentrated in the center of the vessel and is well distributed across the surface by means of the vertical draft tube inlet.

Crystallizers of this type typically operate with a suspension of solids ranging from 25%-50% apparent settled volume. The low temperature drop at the boiling surface and the uniform distribution of boiling created by the circulation pattern minimizes crystallization buildup on the walls of the unit and extends the operating cycle. There are no close clearances where salt buildup can produce a large reduction in the rate of circulation as in other crystallizer designs.

6.1.3.3 Slurry Density Control

SWENSON DTB equipment is especially useful in multiple-stage cooling crystallizer applications where cooling of the feed solution in each stage limits the natural slurry density to a few percent. By means of the baffled zone, the operating slurry density within the crystallizer can be raised to any convenient value by regulating the slurry underflow rate and removing the remaining mother liquor from the baffle section.

Organic and inorganic chemicals produced by the SWENSON DTB Crystallizer include hypochlorite, epsom salt, potassium sulfate, monosodium glutamate, borax, sodium carbonate decahydrate, trisodium phosphate, sodium chlorate, boric acid, MAP, urea, YP soda, etc.

Basic principles of the SWENSON DTB Crystallizer are as follows:

- Growing crystals are brought to the boiling surface where supersaturation is most intense and growth is most rapid.
- The baffle permits separation of unwanted fine crystals from the suspension of growing crystals, thereby affecting control of the product size.
- Sufficient seed surface is maintained at the boiling surface to minimize harmful salt deposits on the equipment surfaces.
- Low head loss in the internal circulation paths makes large flows at low power requirements feasible.

Advantages of the DTB Crystallizer are as follows:

- Capable of producing large singular crystals.
- Longer operating cycles.
- Lower operating costs.
- Minimum space requirements, single support elevation.

- Adaptable to most corrosion resistant materials of construction.
- Can be easily instrument controlled.
- Simplicity of operation, startup and shutdown.
- Produces a narrow crystal size distribution for easier drying and less caking.
- The product size varies only slightly with large changes in production rate.

6.1.3.4 Direct Contact Refrigeration Crystallization

When crystallization occurs at such a low temperature that it is impractical to use surface cooling or when the rapid crystallization of solids on the tube walls would foul a conventional surface-cooled crystallizer, a DTB crystallizer (or a forced-circulation unit) utilizing the direct contact refrigeration technique can be used.

In this operation, a refrigerant is mixed with the circulating magma within the crystallizer body where it absorbs heat and is vaporized. Refrigerant vapor leaves the surface of the crystallizer similar to water vapor in a conventional evaporative crystallizer. It then must be compressed, condensed, and circulated to the crystallizer to maintain continuous operating conditions. Refrigerants must be relatively insoluble in the solutions processed and have the thermodynamic characteristics to minimize compressor horsepower.

Examples are the crystallization of caustic dehydrate with Freon or propane and that of paraxylene with liquid propane refrigerant.

6.1.3.5 Reactive Crystallization

Reactive crystallization (where a solid phase crystalline material results from the reaction of two components) can often be performed more profitably in a crystallizer than in a separate reactor. An example of reactive crystallization is the production of ammonium sulfate from liquid or gaseous ammonia and concentrated sulfuric acid.

The DTB crystallizer is particularly suited for reactive crystallization. The reactants are mixed in the draft tube of the DTB unit where a large volume of slurry is mixed continuously with the materials to minimize the driving force (supersaturation) created by the reaction. Removal of the heat produced by the reaction is accomplished by vaporizing water or other solvents as in a conventional evaporative type crystallizer.

Reactive crystallization can also be performed in a forced-circulation-type crystallizer where the reactants are mixed in the circulation piping.

6.2 **GEA Process Engineering Division**

The Process Engineering Division (P-Division) of GEA is a world leader in spray drying, fluid bed drying, and liquid processing. Core companies in the group are Niro A/S in Copenhagen, **Niro Inc. in Columbia, Maryland/Hudson, Wisconsin, USA**, and the Tuchenhagen Group in Büchen, Germany. <http://www.niroinc.com/html/niro.html>

Their work focuses on the crystallization of solutions and not on the melt crystallization. Their expertise covers the three types of crystallization process:

- By concentration.
- By cooling (under vacuum or with a heat exchanger).
- By reaction or equilibrium displacement.

They possess the know-how and expertise for all types of crystallization equipment with total or partial classification, involving the recirculation of the magma, with or without settling zones.

Crystallizers from GEA Evaporation Technologies (GEA Kestner) include the following types:

- Forced Circulation Crystallizer
- Oslo Type Crystallizer (classified-suspension crystallizer)
- DTB Crystallizer (draft-tube-baffle crystallizer)
- Induced Circulation Crystallizer

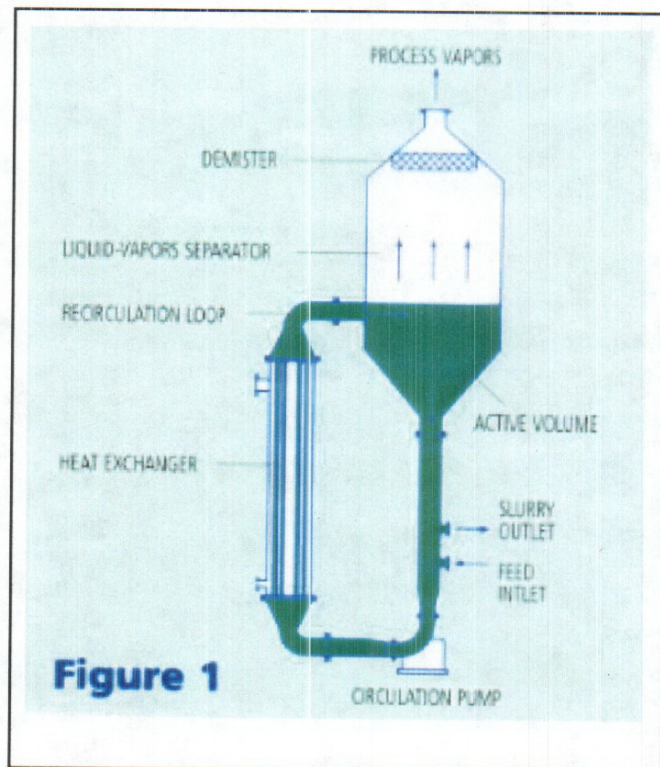
Note: The following is a reproduction of information on the GEA website.

6.2.1 Forced-Circulation Crystallizer

Forced Circulation Crystallizer

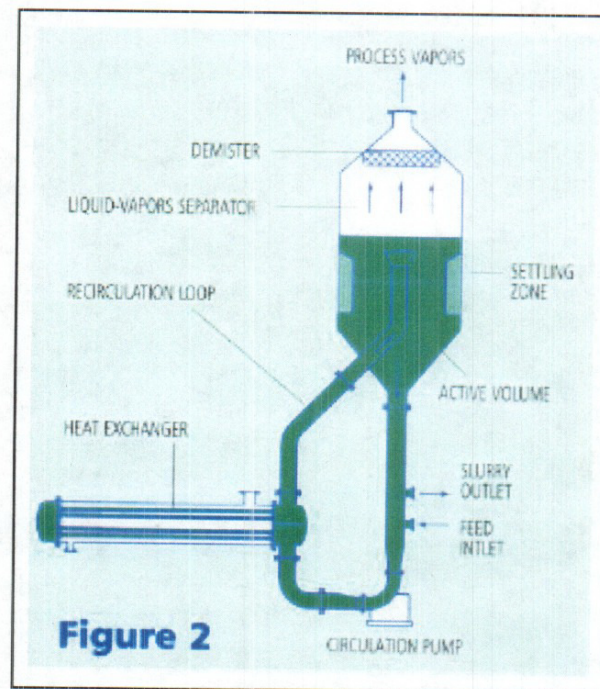
Figure 1 shows a continuous forced circulation crystallizer. It is much like a simple forced circulation evaporator, but it includes specific features to allow correct crystallization, namely:

- an "active volume", designed case by case, to get both required residence time for crystal growth and mother liquor desupersaturation;
- a given agitation (recirculation rate) rated to control the extent of supersaturation arising from the evaporation, and to keep the temperature difference in the heat exchanger within reasonable limits;
- a special design of the liquid-vapor separation area to minimize the carry over losses and avoid the formation of an excessive amount of fines, which is highly detrimental to crystal growth.



Depending upon specific process requirements, additional devices can be provided. They are:

- internal baffles, used mainly for excess mother liquor overflow and/or withdrawal of fines when crystal growth is slow or disturbed by impurities build-up (see Figure 2),
- elutriation leg, to improve product purity and to deliver a narrow crystal size distribution,
- an internal scrubbing section to reduce the carry over losses, or to provide stripping or absorption devices when a volatile compound must be recovered.



Forced circulation crystallizers are of the (Mixed Suspension Mixed Product Removal) MSMPR type and operate either on controlled or "natural" slurry density depending upon process requirements and/or unit material balance.

These units can be either single or multiple effect and the vapor recompression concept (either thermal or mechanical) is often applied. Usually, they operate from low vacuum to atmospheric pressure.

As a rule, these units are used for high evaporation rates and when crystal size is not of the utmost importance or if crystal grows at a fair rate. Almost any material of construction can be considered for the fabrication of these crystallizers. Also, the heating element is omitted for vacuum cooling crystallizers.

Typical products are:

- NaCl (food or technical grade)
- KNO₃
- Na₂SO₄, K₂SO₄
- NH₄Cl
- Na₂CO₃•H₂O
- Citric acid

When the problem of scaling impedes the process of concentration, a design similar to the one described above is proposed. This applies for CaSO₄ saturated solutions, like fertilizer grade phosphoric acid and demineralization effluents.

6.2.2 Oslo-Type Crystallizer

Oslo type crystallizer also called classified-suspension crystallizer is the oldest design developed for the production of large, coarse crystals.

The basic design criteria are twofold:

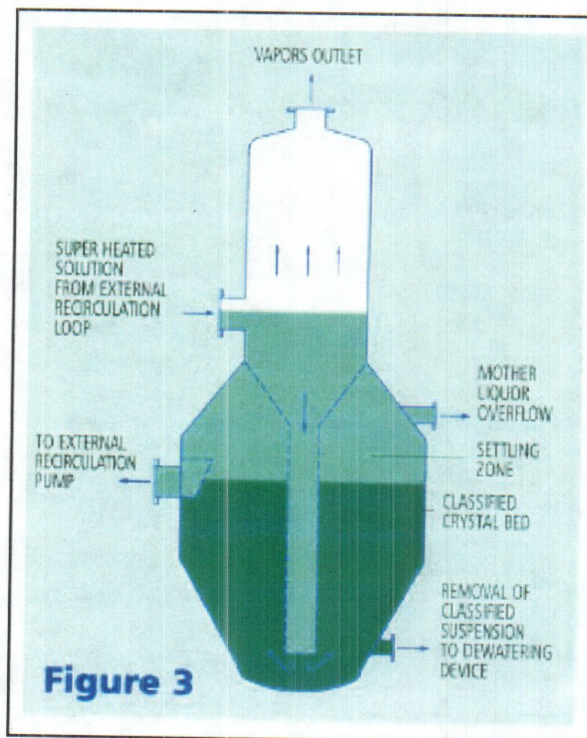
- desupersaturation of the mother liquor by contact with the largest crystals present in the crystallization chamber
- keeping most of the crystals in suspension without contact by a stirring device, thus enabling the production of large crystals of narrow size distribution

The equipment is schematically shown in Figure 3. The classifying crystallization chamber is the lower part of the unit. The upper part is the liquor-vapor separation area where supersaturation is developed by the removal of the solvent (water for most applications). The slightly supersaturated liquor flows down through a central pipe and the supersaturation is relieved by contact with the fluidized bed of crystals. The desupersaturation occurs progressively as the circulating mother liquor moves upwards through the classifying bed before being collected in the top part of the chamber. Then it leaves via the circulating pipe and after addition of the fresh feed, it passes through the heat exchanger where heat make-up is provided. It is then recycled to the upper part.

Additional devices, such as described for the forced circulation crystallizer, are available.

The operating costs of the Oslo type crystallizer unit are much lower than with any other type when both large and coarse crystals are required. Since crystals are not in contact with any agitation device, the amount of fines to be destroyed is lower and so is the corresponding energy requirement.

The Oslo type crystallizer (classified - suspension crystallizer) allows long cycles of production between washing periods.



6.2.2 Draft Tube Baffle Crystallizer

The **Draft Tube Baffle Crystallizer** is an elaborated Mixed Suspension Mixed Product Removal (MSMPR) design, which has proven to be well suited for vacuum cooling and for processes exhibiting a moderate evaporation rate. The concept is such that if no (or little) heat make-up is required, it results in a rather compact arrangement; therefore, the initial investment is minimized.

As a rule, these units operate with a rather low supersaturation, which is sometimes a limitation to crystal growth, so that very large crystals can be produced only by providing extensive and costly dissolving of fines.

The Draft Tube Baffle unit (Figure 5) includes a baffled area (settling zone), peripheral to the active volume, where excess mother liquor and/or fines are removed for further processing. The necessary agitation of the suspension mixed with the incoming feed solution is provided by a bottom entry agitation at moderate energy consumption.

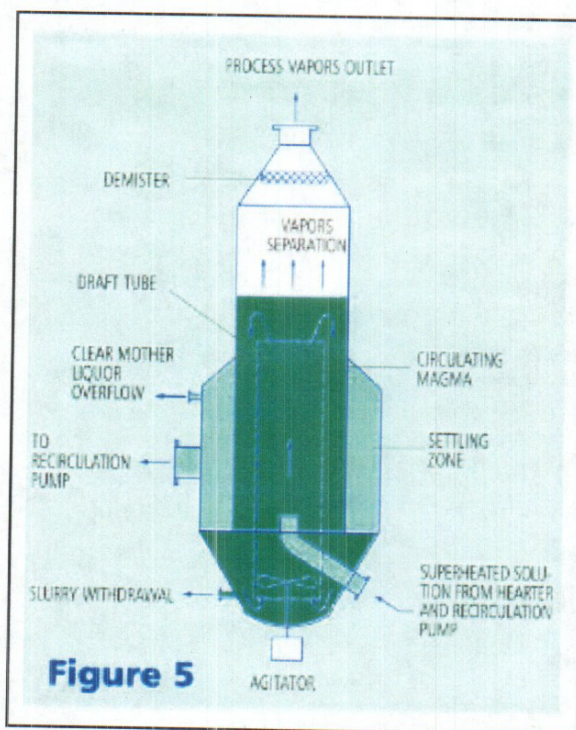
Draft Tube Baffle crystallizers are often equipped with an elutriation leg below the body to classify the crystals.

When destruction of fines is not needed or wanted, baffles are omitted and the internal circulation rate is set to have the minimum nucleating influence on the suspension (Draft Tube design, draft-tube crystallizer).

When large evaporation rates are required, an external heating loop must be provided, making the arrangement less competitive from an initial cost standpoint.

The Draft Tube Baffle Crystallizer, which can be considered when crystallization can be achieved with natural suspension has proven to be well suited to applications such as:

- boric acid
- $\text{Na}_2\text{SO}_4 \cdot 10\text{H}_2\text{O}$ (Glauber salt)
- melamine
- citric acid



6.3 USFilter HPD Systems

Another example is USFilter's HPD Systems, at <http://www.hpd.usfilter.com/Industries>. One example industry is given here.

6.3.1 Chlor-Alkali Evaporation/Crystallization Systems

USFilter's HPD Systems provide evaporation and crystallization systems for the chlorine production brine circuit, product caustic concentration, and production chemicals crystallization.

By controlling brine quality and plant water balance within chlorine/caustic plants, HPD Systems provide brine to the electrolyzer cells to meet stringent requirements. When crystallizing sodium chlorate, HPD Systems meet strict terms on purity and size.

In the soda ash industry, HPD supplies processes for dense soda ash (DSA), light soda ash (LSA), sodium carbonate decahydrate, and sodium bicarbonate. Large, single-effect mechanical vapor recompression (MVR) crystallization systems are used where energy costs dictate.

As a single point of responsibility, HPD offers comprehensive analysis and piloting, process design and development, complete project management and execution, as well as in-depth training and ongoing service.

Chemical Processes

- Caustic potash
- Glauber salt
- Sodium chlorate
- Sodium hydroxide/caustic soda

7. REFERENCES

- Berry, D. A., and K. M. Ng, 1996, "Separation of Quaternary Conjugate Salt Systems by Fractional Crystallization," *AIChE J.*, 42, 2162-74.
- Christensen, S. G., and K. Thomsen, 2003, "Modeling of Vapor-Liquid-Solid Equilibria in Acidic Aqueous Solutions," *Ind. Eng. Chem. Res.* 42, 4260-4268.
- Cisternas, L. A., and D. F. Rudd, 1993, "Process Design for Fractional Crystallization from Solution," *Ind. Eng. Chem. Res.*, 32, 1993-2005.
- Dye, S. R., and K. M. Ng, 1995, "Fractional Crystallization: Design Alternatives and Tradeoffs," *AIChE J.*, 41, 2427-38.
- Dye, S. R., and K. M. Ng, 1995a, "Bypassing Eutectics with Extractive Crystallization: Design Alternatives and Tradeoffs," *AIChE J.*, 41, 1456-70.

- Forshag, W. F., 1935, "Burkeite, a New Mineral Species from Searles Lake, California," *Am. Mineral.* 20, 50.
- Fitch, B., 1976, "Design of Fractional Crystallization Processes Involving Solid Solutions," *AIChE Symp. Ser.*, 72, 153.
- Fitch, B., 1970, "How to Design Fractional Crystallization Processes," *Ind. Eng. Chem.*, 62(12), 6-33.
- Gilbert, S. W., 1991, "Melt Crystallization: Process Analysis and Optimization," *AIChE J.*, 37, 1205-18.
- Green, S., and F. Frattali, 1946, "The System Sodium Carbonate-Sodium Sulfate-Sodium Hydroxide-Water at 100 °C," *J. Am. Chem. Soc.* 68, 1789.
- Guissepetti, G., et al., 1988, "The Crystal Structure of Synthetic Burkeite: $\text{Na}_2\text{SO}_4(\text{CO}_3)_x(\text{SO}_4)_{1-x}$," *Neues Jahrbuch fur Mineralogie, Monatshefte*, 5, 203.
- Hill, C. A., 1981, "Mineralogy of Cave Nitrates," *The NSS Bulletin*, 43, 127-32.
- Helvenston, E. P., et al., 1970, "Double Salt Having the Formula $(\text{Na}_2\text{SO}_4)_4 (\text{Na}_2\text{CO}_3)_9$," U.S. Patent 3,493,326.
- Herting, D. L., 2003, *Test Plan for Tank 241-S-112 Fractional Crystallization Study*, RPP-18541, Rev. 0), CH2M HILL Hanford Group, Inc., Richland, Washington.
- Hightower, J. V., 1951, "The Trona Process and Its Unique Features," *Chem. Eng.*, Aug., 104-106.
- Iliuta, M. C., K. Thomsen, and P. Rasmussen, 2002, "Modeling of Heavy Metal Salt Solubility Using the Extended UNIQUAC Model," *AIChE J.*, 48, 2664-2689.
- Iliuta, M., K. Thomsen and P. Rasmussen, 2000, "Extended UNIQUAC model for correlation and prediction of vapour-liquid-solid Equilibria in aqueous salt systems containing non-electrolytes. Part A. Methanol-water-salt systems," *Chem. Eng. Sci.*, 55, 2673-2686.
- Jongema, P., 1993, "Process of the Preparation of Sodium Chloride," U. S. Patent 5,221,528.
- Krapukhin, V. B., E. P. Krasavina, and A. K. Pikaev, 1997, *Crystallization of Sodium Nitrate from Radioactive Waste*, PNNL-11616, Pacific Northwest National Laboratory, Richland, Washington.
- Linke, W. F., 1965, *Solubility of Inorganic and Metal Organic Compounds*, 4th ed., American Chemical Society, Washington, DC, vol. II.

- Menon, A.R., Kramer, H.J.M., Grievink, J., Jansens, P.J., 2003, "Modelling of growth rate dispersion in industrial crystallizers using a two-dimensional population balance model," *Proceedings of the International Symposium on Process Systems Engineering and Control*, pp.143-148, Bombay, 3-4 January, India
- Mehta, V. C., 1988, "Process for Recovering Lithium from Salt Brines," U. S. Patent 4,723,962.
- Mullin, J. W., 2001, *Crystallization*, 4th ed., Butterworth-Heinemann, Oxford, U. K.
- Mullin, J. W., 1993, *Crystallization*, 3rd ed., Butterworth-Heinemann, Oxford, U. K.
- Neitzel U., 1986, "Neue Verfahren und Projekte zur Herstellung von K₂SO₄," *Kali und Steinsalz*, 9, 257-261.
- Ng, K. M., 1991, "Systematic Separation of a Multicomponent Mixture of Solids Based on Selective Crystallization and Dissolution," *Separations Tech.*, 1, 108.
- Nicolaisen, H., P. Rasmussen, and J. M. Sorensen, 1993, "Correlation and Prediction of Mineral Solubilities in the Reciprocal Salt System (Na⁺, K⁺)(Cl⁻, SO₄²⁻)-H₂O at 0-100°C," *Chem. Eng. Sci.*, 48, 3149-58.
- Purdon, F. F., and V. W. Slater, 1946, *Aqueous Solution and the Phase Diagram*, Arnold, London.
- Rajagopal, S., K. M. Ng, and J. M. Douglas, 1991, "Design and Economic Trade-Offs of Extractive Crystallization Processes," *AIChE J.*, 37, 437-47.
- Rajagopal, S., K. M. Ng, and J. M. Douglas, 1988, "Design of Solids Processes: Production of Potash," *Ind. Eng. Chem. Res.*, 27, 2071-78.
- Schroeder, A., et al., 1936, "Solubility Equilibria of Sodium Sulfate at Temperatures from 150 to 350°. II. Effect of Sodium Hydroxide and Sodium Carbonate," *J. Am. Chem. Soc.* 58, 843.
- Shi, B., Frederick, J. Jr., and R. W. Rousseau, 2003, "Nucleation Growth, and Composition of Crystals Obtained from Solutions of Na₂CO₃ and Na₂SO₄," *Ind. Eng. Chem. Res.*, 42, 6343-47.
- Shi, B., Frederick, J. Jr., and R. W. Rousseau, 2003, "Effects of Calcium and Other Ionic Impurities on the Primary Nucleation of Burkeite," *Ind. Eng. Chem. Res.*, 42, 2861-69.
- Shi, B., and R. W. Rousseau, 2003, "Structure of Burkeite and a New Crystalline Species Obtained from Solutions of Sodium Carbonate and Sodium Sulfate," *J. Phys. Chem.*, B107, 6932-37.

- Shi, B., and R. W. Rousseau, 2001, "Crystal Properties and Nucleation Kinetics from Solutions of Na_2CO_3 and Na_2SO_4 ," *Ind. Eng. Chem. Res.*, 40, 1541-47.
- Sogolov I.D., Ostanina V.A., Safrygin J.S., Rutkovskaja T.I., Antonova N.V., Naginskaja R.E., 1982, "Verfahren zur Herstellung von Kaliumsulfat," Bundesrepublik Deutschland, Patentschrift DE 2820445C3.
- Thomsen, K., and P. Rasmussen, 1999, "Modeling of Vapor-Liquid-Solid Equilibria in Gas - Aqueous Electrolyte Systems," *Chem. Eng. Sci.* 54, 1787-1802.
- Thomsen, K., P. Rasmussen, and R. Gani, 1998, "Simulation and Optimization of Fractional Crystallization Processes," *Chem. Eng. Sci.*, 53, 1551-1564.
- Thomsen, K., 1997, "Aqueous electrolytes: model parameters and process simulation". Ph.D. thesis, Department of Chemical Engineering, Technical University of Denmark.
- Thomsen, K., P. Rasmussen, and R. Gani, 1996, "Correlation and Prediction of Thermal Properties and Phase Behaviour for a Class of Aqueous Electrolyte Systems," *Chem. Eng. Sci.*, 51, 3675-3683.
- Thomsen, K., R. Gani, and P. Rasmussen 1995, "Synthesis and analysis of processes with electrolyte mixtures," *Computers and Chemical Engineering*, 19S, S27-S32.
- Ullmann, 1991, *Ullmann's Encyclopedia of Industrial Chemistry*, Fifth Ed., Wiley-VCH, Vol. A17.
- Xu, T., and K. Pruess, 2001, *Thermophysical Properties of Sodium Nitrate and Sodium Chloride Solutions and Their Effects on Fluid Flow in Unsaturated Media*, LBNL-48913, Lawrence Berkeley National Laboratory, Berkeley, CA.